RSC Advances

REVIEW

View Article Online
View Journal | View Issue

Cite this: *RSC Adv.*, 2024, **14**, 24265

NIR-induced photothermal-responsive shape memory polyurethane for versatile smart material applications

Ki Yan Lam, [a] Choy Sin Lee *[a] and Rachel Yie Hang Tan[b]

Stimuli responsiveness has been an attractive feature of smart material design, allowing the chemical and physical properties of the materials to change in response to small environmental variations. The versatile shape memory polyurethane (SMPU) has been advanced into thermally-responsive SMPU, enabling its use in neurovascular stents, smart fibers for compression garments, and thermal-responsive components for aircraft and aerospace structures. While thermally-induced SMPU materials exhibit excellent shape recovery and fixity, they encounter limitations such as long response times, energy-intensive heating processes, and potential damage to heat-sensitive components, hindering their wide application. Thus, SMPU has further advanced into a photothermal-responsive material by incorporating photothermal agents into the polymer matrix, offering faster response times, compatibility with heat-sensitive materials, and enhanced mechanical properties, expanding the versatility and applicability of shape memory technology. This review focuses on the classes of NIR-induced photothermal agent used in SMPU systems, their synthesis methods, and photothermal-responsive mechanism under NIR-light, which offers a dual responsiveness to the host SMPU. The advantages and limitations of NIR-induced photothermal SMPU are reviewed, and challenges in their development are discussed.

Received 30th June 2024
Accepted 25th July 2024

DOI: 10.1039/d4ra04754k

rsc.li/rsc-advances

[a]*Department of Pharmaceutical Chemistry, School of Pharmacy, IMU University, No. 126, Jalan Jalil Perkasa 19, Bukit Jalil, 57000 Kuala Lumpur, Malaysia. E-mail: choysin_lee@imu.edu.my*

[b]*School of Postgraduate Studies, IMU University, No. 126, Jalan Jalil Perkasa 19, Bukit Jalil, 57000 Kuala Lumpur, Malaysia*

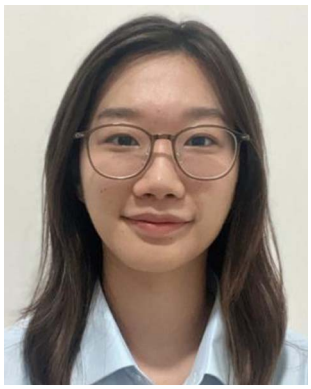

Ki Yan Lam

Ki Yan Lam completed her Bachelor of Science (Hons) in Pharmaceutical Chemistry from the IMU University, Malaysia in 2019. She received her Master of Science (By Research) in Medical and Health Sciences from IMU University, Malaysia in 2023. Following her graduation, she began working as a lecturer at the Department of Pharmaceutical Chemistry, School of Pharmacy, IMU University, Malaysia, continuing her passion for teaching and research. With a strong commitment to both disciplines, she actively engages in imparting knowledge to students while pursuing innovative research endeavors. Her research interests focus on organic synthesis from renewable resources, stimulus-responsive polymers, and exploring their applications in drug delivery systems and biomedical fields.

Choy Sin Lee

Associate Professor ChM Dr Lee Choy Sin holds the position of Associate Dean (Research & Consultancy) at the School of Pharmacy, IMU University. She earned her PhD in Chemistry from the University of Malaya, specialising in palm oil chemistry and polymer chemistry. Boasting over two decades of research experience and 16 years in academia, Dr Lee's expertise centers on the biocompatible and biodegradable polymers derived from renewable resources. Her remarkable contributions include transforming these polymers into pharmaceutical formulations and biomaterials for biomedical applications. Dr Lee has demonstrated her innovation through the filing of two patents in Malaysia and several regional countries, including Singapore, Thailand, Indonesia, and Vietnam.

Introduction

Shape memory polymer (SMP) is a type of smart polymer, in which it is able to interchange from a temporary fixed shape to its original shape when induced by different stimuli such as magnetism,[1] electrical field,[2] and heat.[3] For instance, magnetic-induced SMPs are often employed in electronic devices such as sensors, actuators, and switches. Magnetic-induced SMPs provide precise actuation control, allowing switches to be triggered with accuracy and consistency. When subjected to a specific magnetic field strength, the SMP undergoes a reversible change in shape, effectively toggling the switch between its 'ON' and 'OFF' states. Several studies have reported the use of conductive materials such as carbon fiber felt[4] and electrically conductive silver-ink tracks[5] to enable electrical Joule heating for activating the shape memory effect of SMP without the need for external heating equipment. These electrically driven SMPs are suitable for applications in functional materials and morphing skins.[6] For thermally-induced SMPs, these materials can undergo complex non-linear deformations and changes in thermal boundary conditions, which are driven by phase transitions and segmental rearrangement within the polymer backbone.[7] The thermally-induced SMP has been used in various medical and industrial applications, including intestinal stents,[7] actuators,[8] and sensors.[9]

According to the report published by Grand View Research, the global SMP market size was valued at USD 927 million in 2022 and is expected to reach USD 4770 million by 2030, with a compound annual growth rate (CAGR) of 23.35% during the forecast period.[10] The growing use of the SMP in the medical sector is projected to drive the growth of the SMP market. These SMP materials including epoxy, polylactic acid (PLA) and polyurethane (PU), have distinct features that make them useful in different medicinal applications such as cardiovascular stents, catheter, and orthodontics. Furthermore, the advancement and increase of research and development activities in different sectors around the globe are also expected to drive the market growth.

The PU material segment dominated the global market, accounting for the largest revenue share of over 58% in 2022. This dominance is due to its shape memory properties, outstanding flexibility and elasticity, mechanical strength, and resistance to abrasion, impact, water, oil, and harsh conditions. Thus, shape memory polyurethane (SMPU) is one of the most demanded polymers in shape memory technology. In recent years, thermal-induced SMPU has found extensive utilization across industries, including electronics, automotive,[11] aerospace, textiles,[12] and medical devices[7] due to its unique ability to return to its original shape upon exposure to heat, offering functional and adaptive solutions in diverse applications.

In general, thermal-induced SMPU is made up of two segments: soft segment (SS) that can be used as the reversible phase, while a hard segment (HS) determines the permanent shape at transition temperature (T_{trans}). The hard segments are formed from isocyanates and chain extenders, creating urethane and urea matrices, while the soft segments are composed of polyol chains (Fig. 1i). The T_{trans} of a SMPU can be the glass transition (T_g) of the HS or SS or crystallization temperature (T_m) of the SS. Fig. 1ii illustrates the principles of the temperature induced SMPU. The shape memory behavior of the SMPU can be described in three stages: (1) when $T > T_{trans}$, SMPU can be deformed into a temporary fixed shape by applying mechanical forces, such as tensile or compression forces are applied. During this process, the SS in the polymer

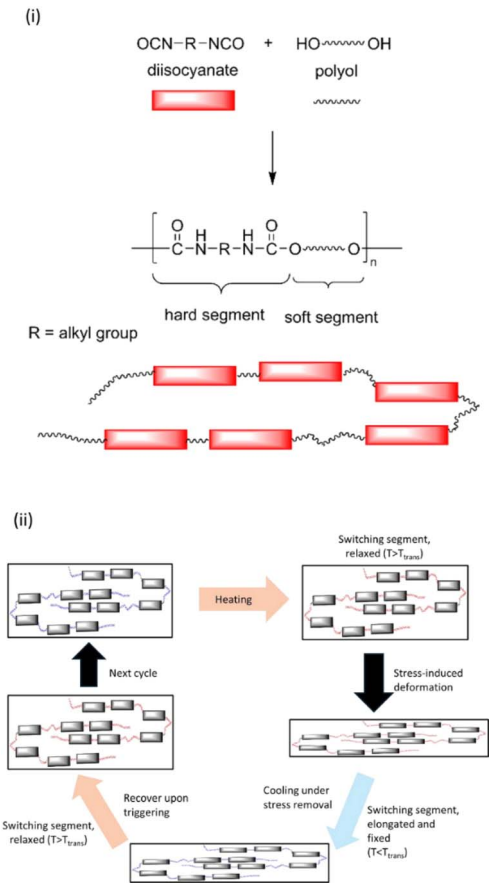

Fig. 1 (i) Reaction scheme of synthesis of shape memory polyurethane and (ii) molecular mechanism of the thermal-induced shape memory effect.

Rachel Yie Hang Tan

Rachel Yie Hang Tan received her BSc (Hons) in Pharmaceutical Chemistry and MSc degree in Medical and Health Sciences (by research) from the IMU University, Kuala Lumpur, Malaysia, in the year 2019 and 2024, respectively. Upon completion of her master's degree, she decided to pursue her PhD in Medical and Health Sciences (by research) at the same university. Her research interests include organic synthesis of polymeric materials from renewable resources, exploring different formulation and their applications in drug delivery systems and biomedical fields.

chains become highly flexible, and the rotations of the soft segment's bonds are becoming significantly greater. This results in a higher entropy state (greater disorder) and an increase in macromolecular conformations. By applying a small loading, the movements of the polymer chain is restricted and thus decrease in the entropy.[13,14] (2) When $T < T_{trans}$, the temporary shape of SMPU is 'memorized' as it reaches the glassy state. The movement of polymer chains is restricted, maintaining the deformation even after the removal of the mechanical constraints. Hence, the temporary shape is obtained even after unloading. (3) Upon reheating, when $T > T_{trans}$, the temporary shape returns to its original shape by releasing the stress and turning the chains into the random orientations again. The polymer chains revert to their random orientations, releasing the stored stress and restoring the high entropy state. This leads to the recovery of the original shape of SMPU.[8]

Polyurethane stands out as a shape memory polymer due to its ability to exhibit shape memory effect in a wide range of shape recovery temperature (−15 °C to 116 °C), processability, biocompatibility as well as good mechanical properties.[7,15,16] The unique composition of soft and hard segments in SMPU contributes to its excellent toughness and tear resistance, making it an ideal candidate for shape memory applications. In addition, the SMPUs can exhibit shape recovery properties over a wide range of temperature, from room temperature to elevated temperature, expanding their potential applications. Due to its exceptional properties, thermal-responsive SMPUs find applications in diverse fields of industrial applications such as actuators,[17] sensors,[18] robotics and aerospace,[19] smart textiles used in smart clothing which can regulate moisture and heat transfer to the wearer's body.[20]

The biocompatibility and flexibility of SMPU make it a promising material for biomedical devices, particularly in self-expanding vascular stents. However, SMP-based stents often face challenges such as insufficient radial support after shape recovery and limited support in narrow vessel, significantly hindering their practical use.[21] To address these issues, Yang *et al.* (2022) synthesized a series of SMPU with full hard segments on the main chains and hydrophilic tertiary amine soft segments on the side chains.[22] In water, the tertiary amine side chains in SMPU enhanced its water absorption and hydrophilicity, as demonstrated by improved hemocompatibility and promotion of cell growth and adhesion (human umbilical vein endothelial cells). Meanwhile, immersion of SMPU in water at 37 °C triggered a soft-to-stiff transformation due to segmental rearrangement and thus significantly increasing its Young's modulus to 345 MPa. These properties are essential for vascular stents as well as maintaining high recovery ratio under physiological conditions is crucial to minimize damage to the blood vessel wall during deployment.

In the work of Zeng *et al.* (2020), thermal-induced shape memory polyurethane (TSMPU) was prepared by blending commercially available polyester-based thermoplastic polyurethane (TPU) and poly(propylene carbonate) (PPC).[23] PPC with a T_g of 33 °C, acts as a switchable phase to activate the thermo-mechanically programmed shape. TPU functions as a rubbery material to prevent PPC from damage under high deformation by locally releasing stress and dissipating energy. TPU also offers superior recoverability, allowing it to memorize its original phase, and restoring the permanent shape. At room temperature, thermally stretched TSMPU tends to recover its shape, aided by the elastic properties of TPU storing the deformation energy, while the strain is primarily preserved by the mechanical support of the glassy PPC. At 37 °C ($T > T_g$), the TSMPU gradually recovered to its original shape with a recovery ratio of 90% in 10 min. The incorporation of TPU enhanced the deformability of PPC, leading to improve shape memory effects.

In the study of Staszczak *et al.* (2022), thermoset SMPU films showed a slower recovery rate, taking 30 min to return to their original shape.[8] Nevertheless, the prepared SMPU films demonstrated excellent shape fixity (R_f) and shape recovery (R_r) of ∼98% and ∼93%, respectively. Another SMPU foam prepared by Kumar and co-researchers (2019), also exhibited nearly 100% recovery after reheating the foam above T_g (24 °C).[3]

While thermal-induced SMPU exhibits excellent shape recovery and fixity, they also encounter several limitations. Notably, thermal-induced SMPU often demonstrates long response time, affecting the speed of shape recovery, especially for thick or insulating materials.[24,25] In addition, transitional heating methods often require energy-intensive process, leading to inefficiencies, higher cost in manufacturing, and potential compromises in mechanical properties due to thermal stress.[26,27] The compatibility of SMPUs with heat-sensitive components also poses a significant concern, as the thermal activation process may risk damaging such materials or components, thereby limiting their application in certain industries. Low recovery stress, modulus and stiffness in thermal-induced SMPU are the main obstacles for their widespread applications.[24] To address these challenges, researchers have turned to the development of light-induced photothermal-responsive SMPU, offering faster response times and compatibility with heat-sensitive materials, remote precise control over heating and thus expanding the versatility and applicability of the shape memory technology. Incorporation of photothermal agent into SMPU matrix not only enhances the mechanical properties and recovery stress of SMPU, but also produces multifunctional composites. Besides, superior H-bonding in neat PU has been associated with longer shape recovery time against thermal stimulation, in comparison to PU composite with addition of photothermal agent.[28]

In this review, different types of NIR-induced photothermal agents used in SMPU are discussed. The synthesis and characteristics of photothermal-responsive SMPUs are reviewed. Despite the advancement of the photothermal-responsive SMPU, we also decipher the limitations and challenges associated with photothermal-responsive SMPU. Future prospects of the photothermal-responsive SMPU are discussed.

NIR-induced shape memory polyurethane with photothermal effect

In contrast, light stimulus offers the benefit of clean, remote control, localized and quantitative selection. The wide range of wavelength from ultra-violet (UV, $\lambda = 200–400$ nm), visible light

Table 1 Summary of NIR light-induced photothermal-responsive shape memory polyurethanes from 2018 to 2024 (searches done on https://Scopus.com, date: 18th May 2024)[a]

Form of SMPU	Photo-thermal agent (optimal amount used in the SMPU)	Polyol	Poly-isocyanate	Preparation method of SMPU	NIR light exposure (λ and power)	Temperature-induced shape recovery	Shape recovery time	Unique features	Application	Ref.
Fiber	Polydopamine (1.1 g mL^{-1} with 12 h immersion)	PCL-2000	IPDI	Electro-spinning	808 nm; 0.2–1 W cm^{-2}	45 °C	18 s in 1 W cm^{-2}	R_r > 96%; increased hydrophilicity; PDA enhanced the focal adhesion of cells	Bone repairing and healing	31
Film	Polydopamine particle (0.01 wt%)	Commercial thermoplastic ether type SMPU (MM-7520)		Extrusion	808 nm; 1 W cm^{-2}	95 °C	60 s	Rapid rise of temperature to 134 °C in 37 s; increased modulus (1.63 MPa to 2.45 MPa); R_f and $R_r \approx$ 99%	Skin care patch	32
Film	Polydopamine particle (0.17%)	PCL-2000	HDI	Solvent-casting method	808 nm; 0.33 W cm^{-2}	60 °C	—	High dispersity; excellent mechanical properties (tensile stress = 10.8 MPa, elongation at break = 1505%); R_f and R_r >98%; shape memory performance up to 5 cycles	Biomedical implant	33
Sponge	Polydopamine particle	Commercial PU sponges		Direct immersion	808 nm; 0.32 W cm^{-2}	70 °C	25 s	Improved hemostatic effect; R_r >80%; increased compressive stress (40 kPa to 71 kPa); improved mechanical properties (tensile strength = 855 kPa, Young's modulus = 580 kPa)	Hemostatic material	34
Film	Black phosphorus crystals (0.08 wt%)	PLA	HDI	Solvent-casting method	808 nm; 0.17 W cm^{-2}	60 °C	50 s	Shape memory performance up to 5 cycles; effective photothermal conversion (increased by 47 °C in 5 min)	Implant device (fallopian tube contraceptive material)	29

Table 1 (*Contd.*)

Form of SMPU	Photo-thermal agent (optimal amount used in the SMPU)	Polyol	Poly-isocyanate	Preparation method of SMPU	NIR light exposure (λ and power)	Temperature-induced shape recovery	Shape recovery time	Unique features	Application	Ref.
Scaffold	Magnesium particle (4 wt%)	PCL-5000	MDI	3D printing	808 nm; 1 W cm^{-2}	80 °C	100 s	Shape memory performance up to 6 cycles; R_f = 83%; R_r = 95%; improved mechanical properties; (tensile strength = 6.7 MPa and Young's modulus = ~23.0 MPa); osteopromotive performances; the scaffold lifted a 100 g weight (1700× of its weight) under NIR light	Robust bone generation	35
Film	Gallic acid-ferric ions chelate (0.3 wt%)	PBA-2000 and PEGB-1000	IPDI	Direct mixing	808 nm; 0.8 W cm^{-2}	60 °C	40 s	Shape memory performance up to 3 cycles; $R_r \approx$ 100%; improved electrolyte stability of nonionic GWPU dispersion allowing GA-Fe nanoparticles with good compatibility to be well dispersed	Actuators	36
Film	Graphene oxide	ε-CL	MDI	Solvent-casting method	λ: —; 1.4–2.5 W cm^{-2}	90 °C	—	Shape memory performance up to 7 cycles; R_r and R_f > 95%; self-healing properties	Actuators; self-healing coatings optical welding materials	37
Film	Multi-functionalized graphene oxide (2 wt%)	PHA-2000 and PTMG-2000	TDI	Two-step method involving de-hydration of reagents and solvents followed by polymerization	400–1100 nm; power: N/A	45 °C	180 s	Self-healing; R_r and R_f > 90%; shape memory performance up to 3 cycles; flame retardancy (LOI: 24.9%; UL-94: V-2 (burning stops within 60 s)); water resistance	Stimulus-responsive composite materials with versatile functions	38

Table 1 (*Contd.*)

Form of SMPU	Photo-thermal agent (optimal amount used in the SMPU)	Polyol	Poly-isocyanate	Preparation method of SMPU	NIR light exposure (λ and power)	Temperature-induced shape recovery	Shape recovery time	Unique features	Application	Ref.
Film	Reduced graphene oxide (2 wt%)	PHA-2000 and PTMG-2000	TDI	*In situ* polymerization	800–1100 nm; power: —	50 °C	6 s	Shape memory performance up to 3 cycles; R_r = 94%; R_f = 92%; self-healing properties	Thermoset shape memory composite materials	39
Film	Diglycidyl ether-functionalized graphene oxide (2 wt%)	PCL-3000	MDI	Solvent-casting method	808 nm; 3.8 W cm^{-2}	55 °C	5 s	Shape memory performance up to 5 cycles; R_r and R_f = 98%; enhanced thermal stability (T_{max} = 405 °C) and mechanical properties (modulus = 48.96 MPa)	Actuators	40
Film	Carbon nanotube	PEG-52000	HDI	Solvent-casting method	980 nm; 1.41 W cm^{-2}	120 °C	120 s	R_f > 98%; R_r = ~100%	No specify	41
Film	Boron-doped single-walled carbon nanotubes (3 wt%)	PTMG-1800	MDI	Solvent-casting method	808 nm; 1.5 W cm^{-2}	20 °C	—	Self-healing properties; rapid increased temperature to 250 °C in 10 s; R_r = 63%; R_f >99%	Electronic devices heat-generating coating material (deicing of airplane)	42
Film	Oxidized carbon black (0.75%)	PCL-4000	HDI	Solvent-casting method	808 nm; 2.0 W cm^{-2}	60 °C	20 s	Enhanced mechanical properties (tensile strength = 20 MPa and Young's modulus = 167 MPa); R_f and R_r ≈ 100%; enhanced biodegradability (>20% than neat SMPU)	Intestinal stents	43
Film	Nanocarbon spheres (0.5 wt%)	PTMG-250 and PTMG-1000	IPDI	Solvent-casting method	808 nm; 3 W cm^{-2}	80 °C	60 s	Anti-corrosion; self-healing properties; reduction in mechanical properties (tensile strength = 8.42 MPa and elongation at break = 194%)	Self-healing and anti-corrosive coating	44
Fiber	Polyaniline	PEO-100000 and PPG–PEG–PPG-2000	TDI	Electro-spinning	808 nm; 1.5 W cm^{-2}	70 °C	500 s	Anti-corrosion; self-healing properties	Anti-corrosive coating	45

Table 1 (*Contd.*)

Form of SMPU	Photo-thermal agent (optimal amount used in the SMPU)	Polyol	Poly-isocyanate	Preparation method of SMPU	NIR light exposure (λ and power)	Temperature-induced shape recovery	Shape recovery time	Unique features	Application	Ref.
Film	1,4-Benzoquinone dioxime	Castor oil-based polyol	HMDI	Hot pressing	808 nm; 0.8 W cm^{-2}	70 °C	<30 s	Antibacterial; R_f and R_r > 90%; rapid increased temperature to 102.1 °C in 50 s under NIR light	Robots; intelligent machinery; sterilization equipment	46
Film	Melanin (2 wt%)	PU pellets (ChronoFLex C 80A)		Solvent-casting method	808 nm; 0.5 W cm^{-2}	90 °C	60 s	Laser intensity lower than photothermal cancer therapy; shape memory performance up to 5 cycles	Implant	47

[a] HDI: hexamethylene diisocyanate; HDMI: hexamethylene diisocyanate; IPDI: isophorone diisocyanate; LOI: limiting oxygen index; MDI: methylenebis(phenylisocyanate); PBA: poly-1,4-butylene adipate glycol; PCL: poly(ε-caprolactone) diol; PEG: poly(ethylene glycol); PEGB: polyethylene glycol branched diol; PEO: polyethylene oxide; PHA: poly(hexylene-adipate) diol; PLA: polylactic acid; PPG: poly(propylene glycol), PTMG: polytetramethylene ether glycol; R_f: shape fixity; R_r: shape recovery; TDI: 2,4-toluene diisocyanate.

(Vis, λ = 400–700 nm) to near-infrared light (NIR, λ = 780–1100 nm), broadens the application area of light-induced SMPU to a larger extent.[29] Particularly, infrared (IR) light encompasses a broader spectrum, including NIR, mid-infrared (MIR, λ = 1300 nm to 3000 nm), and far-infrared (FIR, λ = 3000 nm to 1 nm) lights, offering flexibility in triggering SMPU materials with different compositions and thicknesses. Infrared lasers emit precise wavelengths within the NIR or IR spectrum, providing focused beams for localized heating and high spatial resolution. In this case, NIR light is widely employed in biomedical application due to its excellent tissue penetration ability and tissue harmless.[30] Out of 42 published articles (**https://Scopus.com** with the keywords of light/photo, photothermal, and shape memory polyurethane; years: 2018 to 2024; dated 18th May 2024), 35 articles are reporting on NIR-induced photothermal-responsive SMPU; other publications are reporting on UV light (1 article), visible light (1 articles), VIS-NIR (1 article), UV-Vis-NIR (2 articles) and 2 articles with no reported wavelength of light. NIR light sources are known to be highly efficient, providing sufficient energy for triggering shape memory effect while reducing energy consumption.[26] This is crucial for large-scale industrial application where energy costs are a significant factor. Thus, this review focuses on NIR-induced photothermal-responsive SMPU.

Table 1 summarizes the photothermal agents used in SMPU and their corresponding NIR light wavelength and temperature. Most of the reported SMPU materials are appear in the form of PU film,[29,32,33,36,47] while some are in fiber,[31,45] sponge,[34] and scaffold forms.[35] Poly(ε-caprolactone) diol and aliphatic or aromatic polyisocyanate are commonly used as starting reactants for the SMPU synthesis. Photothermal conversion in these SMPUs typically falls within the NIR light range, inducing a temperature increase that facilitates shape recovery within the range of 45 to 120 °C. This process yields efficient shape recovery ratios (R_r) and shape fixity (R_f) value (>80%). These SMPUs also exhibit shape recovery time of less than 120 s. The deep penetration and non-toxic nature of NIR light highlighted the huge potential of biocompatible SMPU for a wide range of applications, particularly in medical and biomedical fields. Section 2 discusses SMPU prepared using various photothermal agents, including polydopamine, inorganic particles, graphene oxide, other carbon-based photothermal agents, and natural photothermal agents.

Polydopamine photothermal agent-containing SMPU

Dopamine (DOPA) is a natural metabolite of 3,4-dihydroxyphenylalanine, which is found in adhesive proteins in mussel.[48] In basic conditions, catechol group of dopamine is oxidized and thus self-polymerized to form polydopamine (PDA) *via* radical-induced pathway (Fig. 2).[50] The polydopamine particles (PDAP) was reported with higher photothermal conversion efficiency[51–53] and photostability[53] in which it has a higher photothermal conversion efficiency than other photothermal agents.[54] The PDAPs also exhibit better photostability

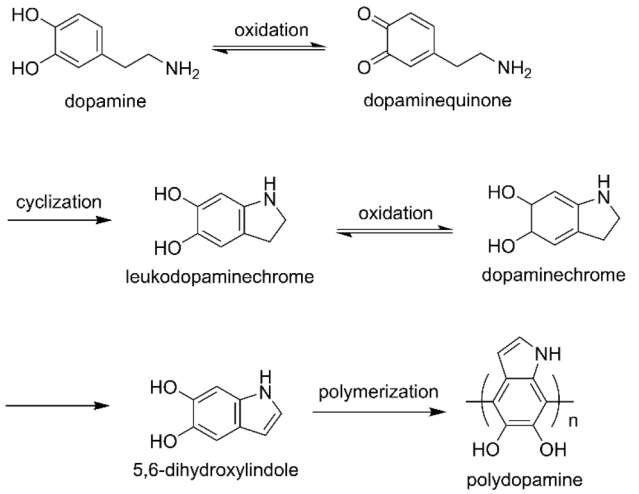

Fig. 2 The self-polymerization of polydopamine.[49]

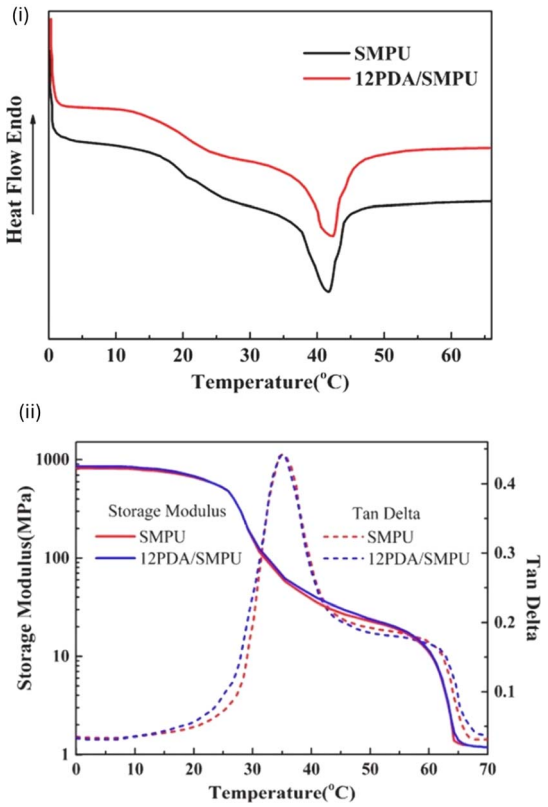

Fig. 3 (i) DSC curves and (ii) tensile storage modulus and tan δ trace measured by DMA of SMPU fibers and SMPU/PDA fibers. Reprinted with permission.[31] Copyright 2021, Elsevier.

than AuNP as it able to absorb more light energy and convert it into heat by NIR exposure.[32,53]

The conjugated structure of indole-quinone and the electron donor–acceptor structures between 5,6-dihydroxyindole synergistically provides PDA a wide range of light absorption.[55] Studies showed that the PDA able to convert 99% of the absorbed photo energy to heat within 50 ps.[56] Moreover, the PDA also able to increase local temperature of the polymer to achieve the shape recovery at a low PDAPs content. The PDAPs interact with PU *via* hydrogen bonding and resulting in enhancement of mechanical properties of PU.[32,57] By considering the excellent photothermal effect, chemical active multifunctional groups and green chemistry availability of polydopamine, PDAPs have been used as a filler to fabricate SMP.

Lv *et al.* (2021) developed a cytocompatible SMPU with photothermal effect.[31] The SMPU was synthesized by reacting isophorone diisocyanate (IPDI), PCL (M_n = 2000 g mol^{-1}) and 1,4-butanediol chain extender by step addition polymerization. The photothermal SMPU fiber was fabricated by electrospinning of SMPU in DMF and further coated with PDA-containing solution to obtain the PDA/SMPU fiber. PDA acted as a photothermal agent and their photo-responsiveness was transferred to the host SMPU fibers. From differential scanning calorimetry (DSC) and dynamic mechanical analysis (DMA) analyses (Fig. 3), the synthesized PDA was not affected much on the thermal behavior and mechanical properties of SMPU under different thickness of PDA coating. The photothermal shape memory properties were evaluated by a bending method. The SMPU samples were first bent to U-shape and fixed in liquid nitrogen and subsequently shined under NIR light (808 nm, LASEVER, China) with different light intensity. SMPU/PDA required minimum light intensity (>0.2 W cm^{-2}) to demonstrate photothermal-induced shape memory effect. The results suggested that more heat could be generated locally with the increased intensities, suggesting the tunable heat from PDA coatings of SMPU fibers resulted from the photothermal conversion with the NIR irradiation. The surface temperature of SMPU/PDA fiber continued to increase as a function of time. When the T (45 °C) > T_m, the shape recovery could be triggered. The highly crosslinked molecular networks were able to provide a strong resilience, which thus would result in relatively faster recovery and higher R_r value (max. 96%). The PDA/SMPU fibers would take 18 s to recover under 1.0 W cm^{-2}. The cytocompatibility evaluation of SMPU/PDA in bone marrow stem cells from Sprague–Dawley rat was also conducted. The SMPU/PDA fibers showed improved cell adhesion and attachment after 3 days of culture. The authors proposed that the synthesized SMPU/PDA is a promising candidate for potential bone repairing and healing.

Yang and co-researchers (2018) reported on the development of a NIR light-responsive SMPU composites by incorporating the synthesized PDAPs[32,58] as photothermal agent into a commercial available SMPU (MM-7520).[32] The mechanical properties of SMPU/PDAPs composites were improved significantly with increasing concentration of PDAPs due to the uniform dispersion and large quantity of active groups on the surface of PDAPs formed strong hydrogen bonding with PU segments and thus the interface interaction between PDAPs and SMPU was improved. The introduction of PDAPs did not reduce the flexibility of the PU when increasing the mechanical properties of SMPU due to the strong cohesion force of PDAPs.[59] The SMPU/PDAPs exhibited dual responsiveness towards NIR light and thermal. The SMPU/PDAPs was elongated to strain at 100% at 95 °C as a temporary shape, which was then being fixed by

cooling to 10 °C before release the stress. When the temporary fixed SMPU/PDAPs was heated to 95 °C again, the SMPU/PDAPs recovered to its original shape. When the SMPU/PDAPs was exposed to NIR light at 808 nm at room temperature, the sample returned to its original unrolled shape. Notably, the shape recovery only occurred at the areas where exposed to NIR irradiation. By exposing to NIR irradiation, the local temperature of PU matrix was increased rapidly above its T_{trans} to achieve the thermal phase transition temperature. The shape memory was achieved at a very low concentration of PDAPs (0.01 wt%) and within a very short period of time (60 s).

Dai *et al.* (2022) synthesized a NIR-induced photothermal-responsive SMPU by reacting PCL (M_n = 2000 g mol^{-1}) and hexamethylene diisocyanate (HDI), followed by the reaction with 1,4-butanediol.[33] The newly synthesized polydopamine nanoparticle (PDANP)[60] was then incorporated as a photothermal agent and chain extender in the SMPU matrix by casting the SMPU and PDANP in THF solution onto a glass fish and left to dry at 40 °C. The synthesized SMPU film with 0.17 wt% of PDANP showed excellent mechanical properties (tensile stress = 10.8 MPa and elongation at break = 1505.3%) due to the PDANP dispersed uniformly in SMPU by the chain extension reaction. However, with a further increase in the PDANP content, both tensile stress at break and elongation at break were reduced. The aggregation of PDANP might has affected the chain extension reaction and reducing molecular weight of crosslinked SMPU, which could further decreased the mechanical properties. The SMPU/PDANP demonstrated its thermal-induced triple shape memory properties (Fig. 4i) by first shaped into a V-shape at 60 °C and fixed at 37 °C to obtain temporary shape A. The V-shape SMPU/PDANP was then deformed into S-shape at 37 °C, followed by fixing in ice bath for 5 min to obtain temporary shape B. When the S-shape sample (temporary shape B) was exposed at 37 °C, it was slowly returned to V-shape (temporary shape A) and remained stable. Finally, the SMPU/PDANP recovered to its initial flat shape at 60 °C. Due

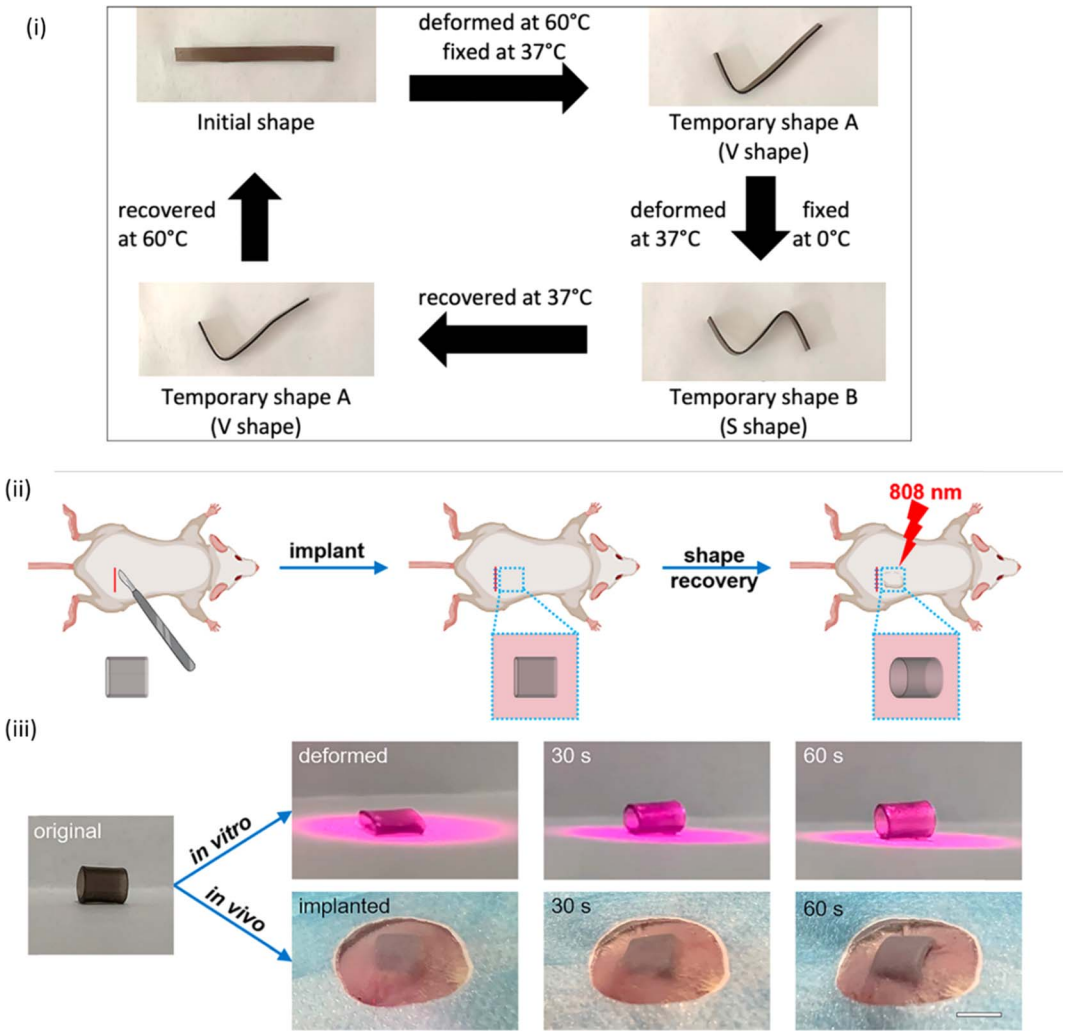

Fig. 4 (i) Digital photographs showing the thermal-induced triple shape memory behavior of SMPU/PDANP; (ii) schematic illustration of *in vivo* shape memory behavior of subcutaneously implanted SMPU/PDANP tubular sample under 808 nm laser and (iii) digital photos of NIR light-triggered shape memory behavior of SMPU/PDANP polyurethane *in vitro* and *in vivo*. Scale bar: 1 cm. Adapted with permission.[33] Copyright 2022, American Chemical Society.

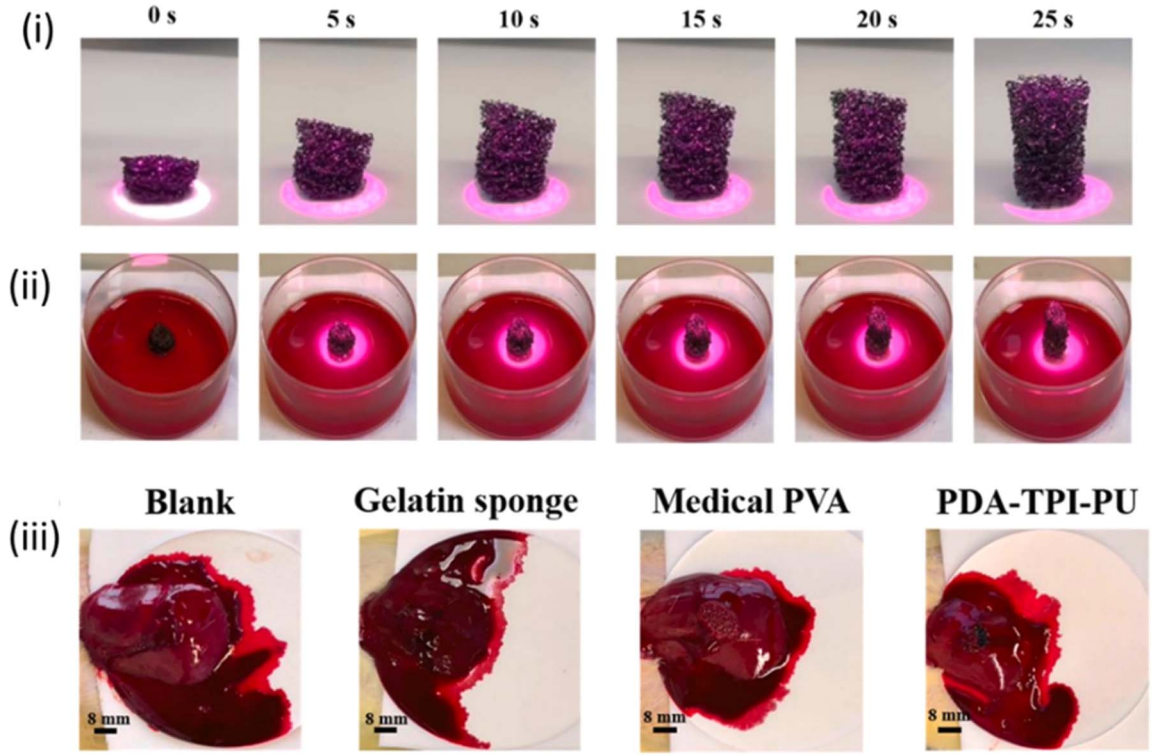

Fig. 5 Photographs showing the NIR light-triggered shape memory behavior of PDA–TPI-PU sponges in the (i) air and (ii) blood under 0.32 W cm^{-2} NIR irradiation. (iii) Photographs of the hemostatic effect of the gelatin sponge, medical PVA sponge, and PDA–TPI-PU sponge. Reprinted with permission.[34] Copyright 2023, Elsevier.

to the excellent tissue penetration of NIR light, the SMPU/PDANP also demonstrated its NIR-induced photothermal shape memory behavior *in vivo* and *in vitro* by implanting SMPU/PDANP in the back subcutis of BALB/c mouse (Fig. 4ii and iii). The tubular sample was first softened and flattened at 46 °C and fixed at 0 °C for 5 min. The temporary fixed sample was then implanted into the back subcutis of the mouse and exposed to 808 nm NIR laser (0.33 W cm^{-2}). Under exposure of NIR light, the temperature of SMPU/PDANP quickly reached over T_m (44 °C) and gradually recovered within 1 min. It is well noted that the NIR light intensity used is the maximum permissible exposure (MPE) for the skin, according to the American National Standard (ANS).[61] The SMPU/PDANP demonstrated high recyclability of photothermal shape memory properties up to 5 cycles of irradiations. The resulted SMPU/PDANP showed excellent mechanical properties (tensile strength = 10.8 MPa and elongation at break = 1505.3%), good *in vivo* biocompatibility (no strong host inflammatory response or damage in any major organs), and NIR light-induced photothermal shape memory behavior, which has a great potential to be used in biomedical implant application.

Sang *et al.* (2023) introduced polydopamine into *trans*-1,4-polyisoprene functionalized commercial SMPU (TPI-PU/PDA) sponge[62] with adjustable degree of expansion under NIR light for the treatment of incompressible hemorrhage.[34] The TPI-PU/PDA sponges exhibited robust mechanical properties and excellent photothermal conversion ability as well as good liquid absorption performance. Under exposure of NIR light (0.32 W cm^{-2}), the prepared PU sponge demonstrated 91% and 80% shape recovery in air and blood, respectively (Fig. 5i and ii). The treatment of hemorrhage was compared with commercial medical gelatin sponge and PVA sponge (Fig. 5iii), the prepared PU sponge could well control the bleeding under NIR light irradiation without over compression of the wound. These results suggested that the TPI-PU/PDA sponge has the potential to be used as a hemostatic material.

Polydopamine (PDA) stands out as a versatile material for offering wide range of temperature that could induce the shape recovery process (45 °C to 95 °C) and improved mechanical properties of SMPU composites. The PDA also demonstrated excellent photothermal conversion ability and efficiency (rapid increased of temperature to 134 °C in 37 s). These characteristics make PDA an ideal filler for SMPU fabrication. In short, the incorporation of PDA into SMPU holds promise for advancing functional materials with enhanced biocompatibility and responsiveness to addition external stimuli, which also demonstrating huge potential to be used in medical and biomedical applications.

Inorganic particle photothermal agent-containing SMPU

The excellent photothermal effect of inorganic particle resulting in strong NIR light absorption and most of them represented dual light- and thermo-responsive in SMPU matrix. As a result, NIR light-responsive SMPU composites have been developed

through incorporating different inorganic photothermal agents such as magnesium, iron, and phosphorus nanosheets into SMPU matrix, resulting in NIR light absorption and followed by light-to-thermal energy conversion.[29,35,36] For instance, black phosphorus (BP) exhibited wide absorption range from UV to IR regions due to its layer-dependent bandgap varying from 0.3 eV (bulk) to 2.0 eV (monolater).[63] The BP nanosheet converts light into heat through photothermal conversion, wherein incident photons excite electrons from the valence bond to the conduction band, generating electron–hole pairs. The majority of absorbed light energy is re-emitted as photons after recombination of electron–hole pairs near the bandgap edge. However, due to non-radiative decay processes, excess energy is release as heat instead of photons. This heat migrates throughout the nanosheet, thus causing localized heating (Fig. 6).[64]

Xie *et al.* (2018) reported on a thermo-responsive SMPU prepared by reacting poly(D,L-lactic acid) (PDLLA) diol and HDI, followed reaction with piperazine as chain extender.[29] The piperazine-containing PU was also incorporated with a synthesized BP nanofiller[29,65] as NIR photothermal agent. Under the NIR light irradiation (808 nm, 0.17 W cm^{-2}), the incorporated BP film with concentration of only 0.08 wt% enabled rapid temperature increased over the glass transition temperature (T_g) of SMPU and triggered the shape changes of the composite and shape recovery rate near to 100% (Fig. 7). The temperature of solution used to disperse the BP nanofiller was increased by 47 °C after 5 min of NIR light irradiation, indicated the BP efficiently converted the NIR light into thermal energy. For the shape memory properties, the SMPU/BP film was heated to 60 °C (above T_g) and bent into half, which was subsequently brought to cool to 4 °C for fixation. The temporary fixed film was gradually recovered to initial shape under NIR light (λ = 808 nm) at room temperature (below T_g). The excellent NIR light responsive shape memory performance is mainly due to the great photothermal conversion of BP nanofiller. The SMPU/BP also demonstrated excellent photostability due to the photothermal efficiency did not decline after 5 cycles. Due to the excellent NIR light penetration and the excellent biocompatibility of SMPU/BP, the resulted polymer was suggested for its potential as implant materials in deeper tissue or as a fallopian tube contraceptive material.

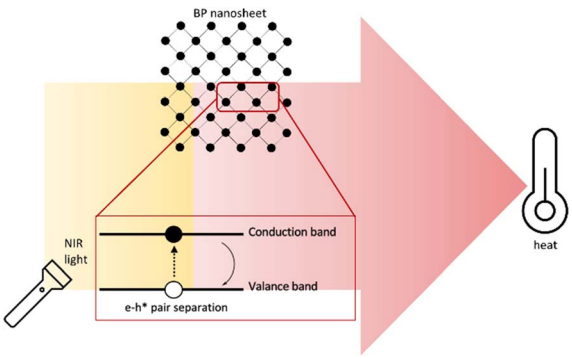

Fig. 6 Illustration of photothermal conversion in black phosphorus nanosheet.

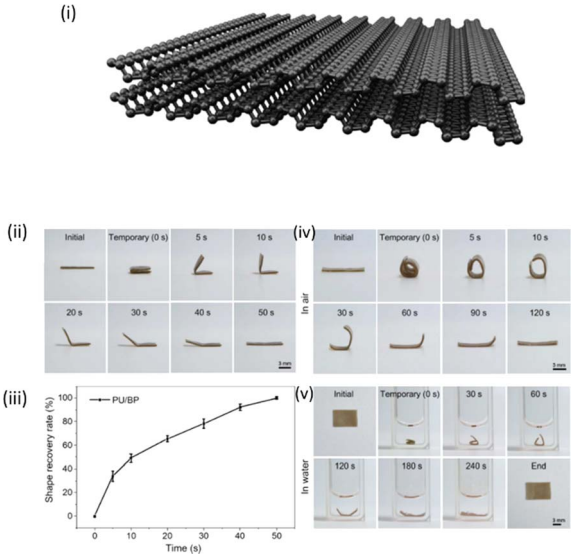

Fig. 7 (i) Schematic illustration of BP sheet; (ii) photographs showing the NIR light triggered shape memory behavior of a folded PU/BP film; (iii) plot of the shape recovery rate *vs.* irradiation time, and photographs showing the NIR light triggered shape memory behavior of a rolled PU/BP film put in (iv) air and (v) water. Reprinted with permission.[29] Copyright 2018, Elsevier.

Patients with bone defects experienced disability and deformity. Conventional treatment for large bone defects is to use bone grafts harvested from the patients or donor, which associated with several limitations from unmatched shape to insufficient osteogenic activities or unsatisfied mechanical performances. While self-expanding scaffold has been developed to improve bone integration, but it has limitations on high T_g and low bioactivity which hindered their clinical application. In the work of Zhang *et al.* (2022), a SMPU/Mg matrix was first prepared by reacting 4,4-methylenebis(phenylisocyanate) (MDI) and PCL-5000 and followed by incorporation of various content of magnesium particle (Mg, 2–8 wt%) into the SMPU matrix to fabricate the photothermal-responsive SMPU scaffold by the low temperature rapid prototyping (LT-RP) 3D printing technology.[35] In their previous study, Mg^{2+} has been proved to promote the neuronal calcitonin gene-related polypeptide-α-mediated osteogenesis differentiation.[35,66] Upon NIR light irradiation (808 nm, 1 W cm^{-2}), especially the SMPU with 4 wt% Mg particles, the SMPU showed optimal performance and excellent photothermal effect by increasing local temperature from 30.0 °C to 67.6 °C ($T > T_m$) within 1 min and achieved R_f of 93.6% and R_r of 95.4%. Due to the excellent shape recovery effect, the SMPU/Mg scaffold could lift an object more than 1700 times heavier than its own weight under NIR light irradiation. The *in vivo* bone regenerative potential of the 3D printed SMPU/Mg scaffold was evaluated by implantation of compressed SMPU/Mg scaffold in calvarial defect of the mouse. The defective skull with the SMPU/Mg scaffold was then irradiated under NIR light (808 nm, 2 W cm^{-2}) for 1 min and the scaffold returned to its initial size with its porous structure. A new bone was found to be formed in the pores of the scaffold due to osteopromotive effect of magnesium ions. These results proved that the 3D printed SMPU/Mg scaffolds had good NIR light-

induced photothermal effect and supporting ability, which makes it a potential material for clinical applications.

In the study of Liu *et al.* (2022), a novel gallic acid waterborne polyurethane (GWPU) with photothermal-induced shape memory property was fabricated by reacting IPDI as hard segments, poly-1,4-butylene adipate glycol (PBA, M_n = 2000 g mol^{-1}) and polyethylene glycol branched diol (PEGB, M_n = 1000 g mol^{-1}) as soft segments as well as BDO as chain extender and gallic acid (GA) *via* stepwise polymerization.[36] For a material to achieve shape memory property, it is required to have a switchable molecular segment and fixed net point. The switching segment is a flexible component responsible for maintaining the temporary shape due to the reversible crystallization, melting or glass transition when external force is applied. Moreover, the net point, which needs to be stable at elevated temperature to maintain the shape of the entire system, is responsible for the memory and recovery of the permanent shape. It is typically formed through chemical or chemical crosslinking or crystallization.[67] The synthesized GWPU film was initially evaluated for its thermal-induced shape memory property by a bending method. The GWPU film was first folded into half and then quickly returned to its original shape upon heating to 60 °C ($T > T_m$). Among the three formulations (Fig. 8ii), GWPU-2 exhibited a recovery ratio of over 94%, indicating excellent shape memory performance. However, GWPU-1 did not show shape recovery property due to insufficient net points formed by the phenol-carbamate network from PEGB and GA.

Gallic acid is a plant polyphenol, which can chelate with ferric ions as a multi-ligand to form self-assemble organometallic complexes (GA-FE) and has strong NIR absorption.[68] Shape recovery performance was investigated on iron gallate (GA-Fe)

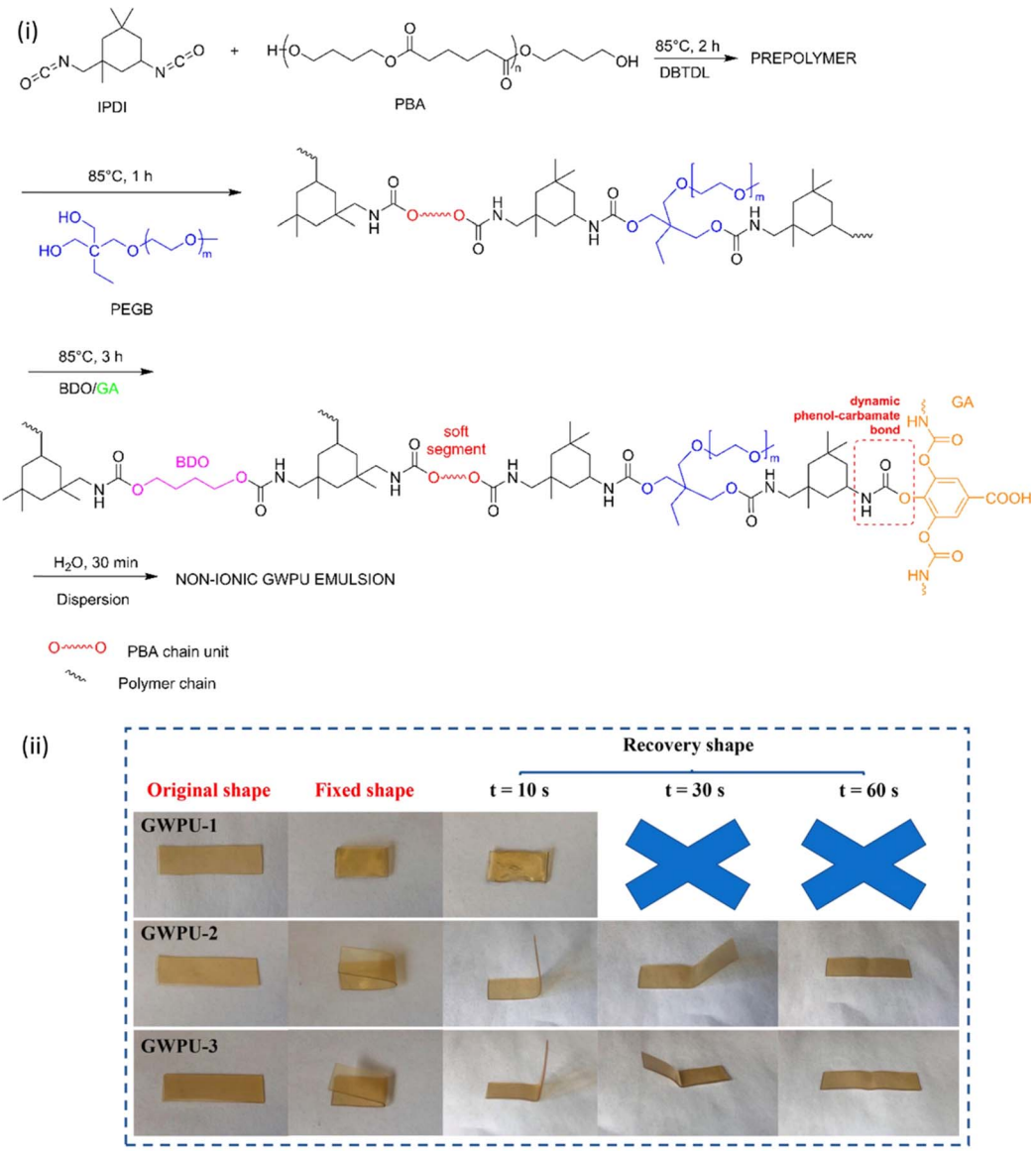

Fig. 8 (i) Reaction scheme of the synthetic route of the non-ionic GWPU dispersions and (ii) photographs of shape memory process of GWPU/GF polymers. Reprinted with permission.[36] Copyright 2022, Elsevier.

nanoparticles. The GA-Fe nanoparticle was prepared by mixing GA solution and $FeCl_3$ solution, followed by incorporation into the GWPU matrix. The synthesized GWPU, especially when the weight content of GA-Fe was 0.3 wt%, it showed excellent mechanical properties because of the GAs were well-dispersed in polymer matrix, as shown by scanning electron microscopy (SEM). Under NIR exposure (0.8 W cm^{-2}), the surface temperature of GWPU/GF rapidly increased from room temperature to 60 °C within 40 s and achieved 100% of recovery ratio. These results demonstrated that GA-Fe nanoparticles possessed an excellent photothermal ability in converting light energy into heat. The authors proposed the prepared photothermal-responsive shape memory GWPU/GF as a smart material in light control actuators.

Metallic nanoparticles have become key components across biomedical and industrial applications. Despite their widespread use, studies have reported that these nanoparticles can induce the release of reactive oxygen species (ROS) and cytokines within the nervous system.[69,70] The extensive application of metallic nanoparticles also increases the exposure risk and potential cytotoxicity to the user.[71] Hence, systematic studies are essential to evaluate the cytotoxicity effect of metallic nanoparticle, particularly in biomedical applications. These studies are crucial for ensuring the safety and efficacy of shape memory polyurethane materials in practical settings.

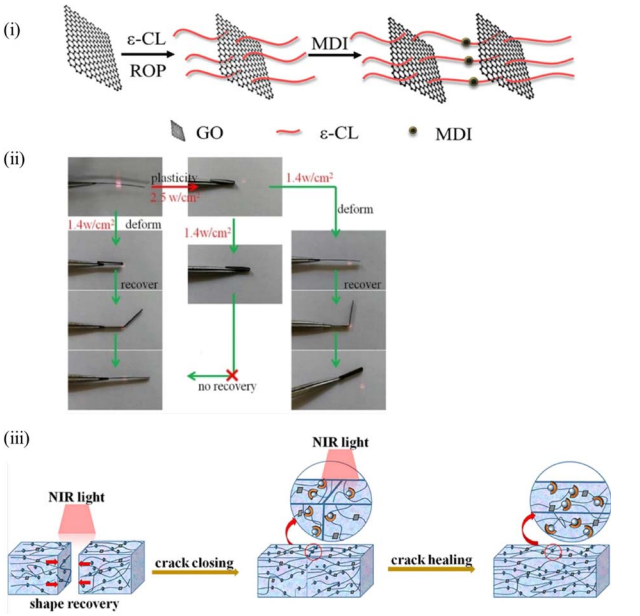

Fig. 9 (i) Synthesis route of GO-SMP; (ii) the photothermal conversion efficiency of GO-SMP and (iii) schematic illustration of the light-induced self-healing process. Readapted with permission.[37] Copyright 2019, Elsevier.

Graphene oxide photothermal agent-containing SMPU

Carbon-based materials have been considered as an effective photothermal agent due to their remarkable features. For instance, graphene has become one of the most studied materials owing to its unique chemical and physical properties, which have suggested its application in electronics, materials science, and biomedical fields.[39,72] In this section, numerous of graphene derivatives are discussed on its advantages to overcome the limitations of graphene, such as poor solubility and high aggregation. Graphene oxide, reduced graphene oxide and other multi-functionalized graphene have been employed as photothermal agent to absorb NIR light to induce shape memory behavior of PU. These graphene derivatives showed satisfactory in solubility, biocompatibility and selectivity.[73]

Bai *et al.* (2020) developed a SMPU/graphene oxide (SMPU/GO) film with light-induced shape memory effect, solid-state plasticity and self-healing properties.[37] The PCL was grafted onto GO by ring opening polymerization of ε-CL and the grafted polymer (PCL-GO) was crosslinked with MDI to build the SMPU/GO network (Fig. 9i). The formation of carbamate (–CO–NH–) was validated between the reaction of MDI and –OH of PCL by FTIR analysis. The produced carbamate was stable at room temperature and could dissociate a small amount of free isocyanate groups at elevated temperature. In addition, the exchange reaction of carbamate provided light-induced plasticity and self-healing properties to the SMPU/GO films due to the photothermal-induced exchange reaction. As a result of the excellent photothermal properties of GO, which endowed the SMPU with the NIR light-induced shape memory effect (SME) and plasticity. Under NIR light irradiation (NIR light wavelength and power: not reported, 1.4 W cm^{-2}), the bent SMPU/GO strip was completely returned to the original straight shape within seconds. The SMPU/GO also reported of its self-healing properties, which is mainly due to the NIR-induced SME of SMPU/GO. The polymer chains diffused across the crack areas along with the carbamate exchange reaction, leading to the topological rearrangement of polymer networks under NIR light exposure (Fig. 9iii). Hence, the NIR-induced self-healing properties of SMPU/GO could be realized with the help of SME. In comparison with thermal-induced SME, the NIR light stimuli could be performed at a controlled, localized and contactless method.[37,74] The authors reported that the temporary and permanent shape of SMPU/GO can be modified by using different power density of NIR light (1.4 to 2.5 W cm^{-2}).

Du *et al.* (2020) synthesized a multi-functionalized GO (mfGO) photothermal agent with phosphorus–nitrogen–silicon-composite and further incorporated it into a diselenide-containing PU (dPTD), which provided the PU with SME and self-healing effect under the exposure of Vis-NIR light as well as enhanced fire safety feature.[38] The mfGO-dPTD composites increased the crystallinity of the polymer and facilitated the shape fixity capability during the shape memory process. The mfGO-dPTD composite with an original shape was heated above the T_g (approximately 45 °C), showing deformation with stretching, circle, and spiral shapes. The deformation was fixed temporarily by cooling to −10 °C. The deformed temporary shapes could almost be recovered to their original shapes under Vis-NIR light (λ = 400–1100 nm) (Fig. 10i). The shape memory mechanism of the mfGO-containing PU involves both crystallization and photothermal behavior. In particular, the mfGO-dPTD composite regions were loosened when heating the PU

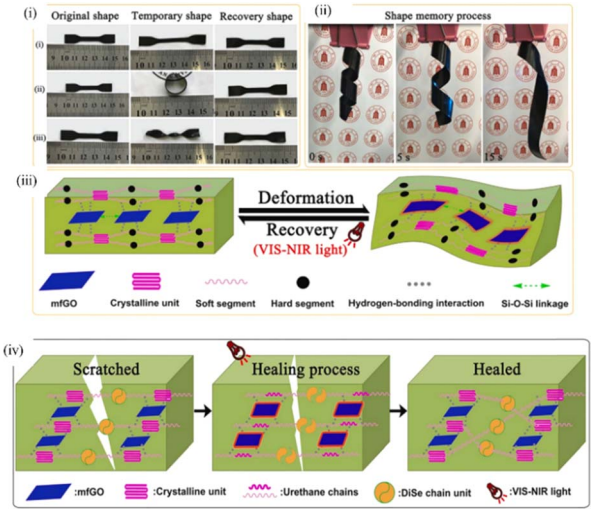

Fig. 10 Shape memory behavior of the mfGO-dPTD composite film. (i) Photographs showing the representative dPTD-mfGO with original shape, temporary shapes (*i.e.*, stretching, circle, and spiral shapes), and recovery shapes; (ii) photographs showing the shape memory process under visible-near infrared (Vis-NIR, 400–1100 nm) illumination.; schematic showing (iii) the mechanism of the VIS-NIR light triggered shape memory behavior and (iv) proposed self-healing mechanism under Vis-NIR light. Reprinted with permission.[38] Copyright 2019, Elsevier.

above the T_g. The temporary shape was fixed during natural cooling due to the nucleation effect of mfGO on PU crystallization. For the recovery process, the thermal energy from Vis-NIR light could be transferred through the PU matrix to melt the crystals and release the temporarily stored strain energy. The graphene could adsorb light energy from the Vis-NIR light and converted it into thermal energy, followed by transferring the energy to the PU matrix to melt the crystals and narrowing the crack surface by the help of shape memory effect. Thus, promoting the interfacial chain diffusion and the rearrangement of diselenide exchange across the damaged surfaces and greatly enhanced the self-healing process (Fig. 10iv).[38,75] The authors expected that the mfGO-dPTD could serve as multifunctional self-healing smart composite materials.

In the same year, Du *et al.* (2020) reported on functionalization of reduced graphene oxide (FRGO) with 2,4-toluene diisocyanate (TDI), in which the urethane linkages achieved better compatibility with PU matrix, with enhanced crystallization behaviors of PU chains and thus improving the shape fixity.[39] The FRGO also formed physical and chemical crosslinking structures in the composite and contributed to the shape recovery process. With 2 wt% of FRGO, the PU demonstrated rapid shape memory ($R_f = 92\%$, $R_r = 94\%$, <10 s) and self-healing effect (<120 s) under exposure of NIR light. It is well noted that the prepared PU/FRGO also showed durable shape memory effect up to three cycles. On the other hand, the furan modified graphene (FGN) acted as effective photothermal agent in maleic anhydride modified PU composite and facilitated the PU film to achieve 100% of shape recovery ratio in 6 s under laser irradiation (600 mW).[76] The FGN also improved the flexibility and voltage of PU making it

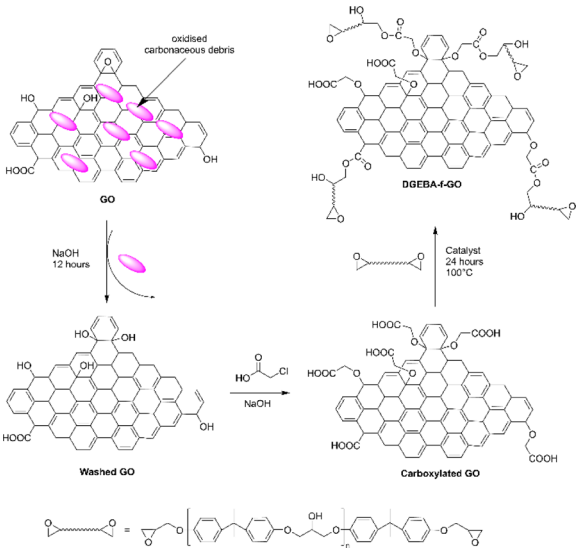

Fig. 11 The reaction scheme of synthesis of DGEBA-f-GO.[40]

a potential candidate for the manufacturing of self-power shape memory motion sensors.

Punetha *et al.* (2019) reported on the enhancement of photothermal performance of GO by removing the oxidized carbonaceous debris complexed prior to functionalization the GO with bisphenol A diglycidyl ether (DGEBA) (Fig. 11).[40] The DGEBA-functionalized GO (DGEBA-f-GO) was then crosslinking with aromatic diamine hardener and epoxide group to form crosslinked networks of the photothermal filler in the PU matrix. The functionalized GO crosslinked networks offered better dispersion and compatibility within the PU matrix to avoid the aggregation of DGEBA-f-GO sheets and hindering π–π interaction. This resulted in more available surface area for interaction with the hard segment N–H bonds of PU.[17] This showed that the crosslinked photothermal networks absorbed NIR light more efficiently by increasing the local temperature to 77.7 °C in 5 s to achieve a rapid shape recovery. These features endow the prepared PU nanocomposites with huge potential in aerospace and biomedical applications, where remote actuation is preferred due to the challenges associated with direct contact control.

Other carbon-based photothermal agent containing SMPU

The properties of any carbon-based materials are depending on their specific structure (shape and size), which is determined by the method of synthesis, experimental conditions and the nature of the carbon source. In addition to functionalized graphene, other carbon-based photothermal agents include carbon black and carbon nanotubes. This section reviews the photothermal-induced shape memory behavior of SMPU containing carbon-based materials and a polymeric photothermal agent, polyaniline.

Yan *et al.* (2017) prepared a novel PU vitrimers–carbon nanotubes (PUV/CNT) with shape memory behavior by reacting

HDI with castor oil and PEG and subsequently introducing the carboxyl multiwall CNT as photothermal filler into the PUV matrix.[41] The incorporation of CNT provided NIR-induced reconfiguration and shape memory properties to PU due to its photothermal characteristics. The introduction of CNT into the PUV as an energy conversion medium converted the NIR light energy into thermal energy to promote thermoplasticity and thus achieved NIR-triggered reconfiguration and shape memory properties. The circular temporary shape was recovered to its original shape under NIR irradiation at 980 nm (Fig. 12ii). It is noteworthy that permanent shape of the PUV/CNT was reshaped into a new permanent shape within 2 min of NIR irradiation and it could not recover to its shape by heat stimulation. When the temperature of PUV/CNT was heated to 120 °C by NIR irradiation for 2 min, transcarbamoylation reaction of carbamate bonds (Fig. 12i) was promoted during the reshaping process. Ha *et al.* (2019) reported that the PU with 3 wt% CNT showed a rapid temperature increased to 250 °C in 10 s.[42] All the SMPU/CNT showed an average R_f > 99% and R_r > 63%. The authors also reported that adding the CNT filler as nucleating agent into the PU has resulted in increased of T_m of soft segment but did not significantly influence the shape memory characteristics.[42] In addition, surface-modified multiwalled carbon nanotubes had overcome the problem of poor compatibility with PU. The hydroxylated MWCNTs form hydrogen bonds with PU, enhancing the self-healing properties of the PU materials.[77]

Studies have highlighted the significant uses of CNTs in various application. However, their cytotoxicity should be taken into consideration. Carbon nanotubes have been demonstrated to induce oxidative stress and inflammation, evidenced by the increased ROS in exposed cells.[78] Different types of CNTs exhibit varying levels of cytotoxicity, depended on factors such as concentrations and functionalization.[79,80] For example, carboxylic-functionalized CNTs have been reported to demonstrate higher cell viability compared to pristine CNTs in neuronal cells, LN18 at concentration up to 40 μg mL^{-1} and after longer incubation period (48 h).[79] Further research into their safe use is required, particularly in medical and biomedical applications.

Pancreas secretes pancreatic juice containing the inactive enzyme chymotrypsinogen, which will activate the chymotrypsin enzyme upon entering the duodenum. Chymotrypsin helps to digest proteins by breaking them down into smaller peptides.[81] Herein, Yang *et al.* (2022) reported a biodegradable PU with NIR light-induced photothermal responsive shape memory property, as a potential implantable material for intestinal stents.[43] A novel chain extender phenylalanine (PHP) derivative with two chymotrypsin cleavage sites was first synthesized.[82] The SMPU was prepared by reacting HDI, PCL-4000 diol, PHP chain extender, and oxidized carbon black (OCB) as photothermal agent (Fig. 13).[43] The carbon black was introduced into the SMPU to provide photothermal-induced shape recovery properties to the PU. In order to enhance the compatibility between SMPU and carbon black, the surface of carbon black was oxidized to increase the carboxyl content, which was conducive to the dispersion of carbon black in SMPU

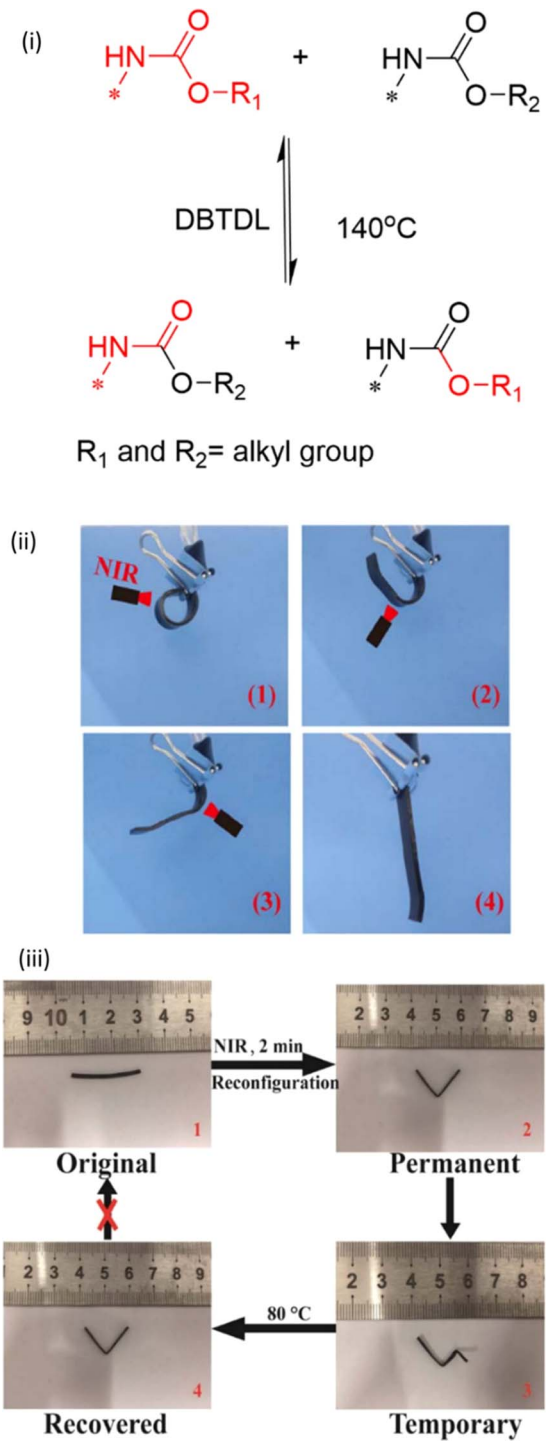

Fig. 12 (i) Reaction scheme of transcarbamoylation; (ii) images of shape recovery triggered by NIR, and (iii) NIR-induced reshaping and partial shape recovery: (1) original shape; (2) reshaped permanent "V" due to NIR-induced transcarbamoylation; (3) the portion on the right was fixed to a temporary shape at lower temperature and (4) heating to above T_m only recovered the portion on the right. Reprinted with permission.[41] Copyright 2017, John Wiley and Sons.

solution in the DMF and SMPU membrane matrix. The OCB served as the physical crosslinking point in SMPU, enhancing the aggregation and interaction of hard segments. Consequently, the T_g of the hard segment and degree of phase

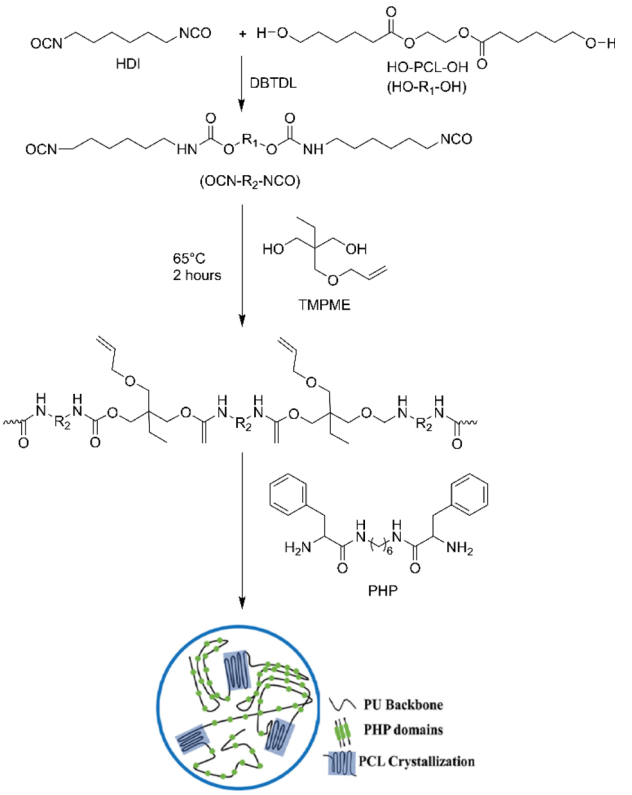

Fig. 13 Reaction scheme of synthesis of biodegradable shape memory polyurethane by reacting HDI, PCL-4000 diol, and phenylalanine (PHP) chain extender. Readapted with permission.[43] Copyright 2022, John Wiley and Sons.

separation increased, which reduced the T_g of soft segments.[83] However, the OCB also acted as a filler uniformly distributed in SMPU, which restricted the chain movements and thereby increasing the T_g of the soft segments.[84] Due to these two factors, T_g of soft segments remained unchanged. Self-expanding intestinal stents are relying on the shape memory effect of the smart material due to the mild mechanical stimulation to the lumen wall.[85] When T_{trans} (55 °C) was higher than the body temperature (37 °C), the SMPU was capable to achieve shape recovery through photothermal conversion for intestinal stents after implantation. The SMPU/OCB was folded at 60 °C and then cooled at −20 °C to temporarily fix the shape. Under NIR light exposure (808 nm, 2.0 W cm^{-2}), the SMPU/OCB film began to unfold due to the photothermal effect of OCB, achieving close to 100% shape recovery in 20 s when the temperature (60 °C) exceeded the transition temperature (T_{trans}). Moreover, certain clinical applications of intestinal stents necessitate surgical removal due to their non-degradable nature.[86] Enzymatically degradable intestinal stents could relief patient discomfort by enabling *in vivo* degradation after providing mechanical support to the lumen. In this study, the prepared SMPU/OCB films were degraded by chymotrypsin, an enzyme found in pancreatic juice, with an adjustable degradation rate. The SMPU/OCB films exhibited excellent shape memory effect, rapid photothermal response and adjustable biodegradability, demonstrating its great potential as a smart biomaterial for short-term use in intestinal stents.

Nevertheless, it is well noted that the OCB provided excellent photothermal conversion. Meanwhile, OCB also acted as a filler distributed uniformly in SMPU, which restricted the movement of the chain segments and increased the T_g of the soft segments.[43,83] The T_g is a critical parameter that influences various aspects of material performances in biomedical devices, such as mechanical properties, shape memory performance, and processing conditions.

In the work of Zhang *et al.* (2024), a SMPU matrix was prepared *via* solution polymerization method.[44] Then, reversible quadruple hydrogen bond (UPy) was synthesized using a one-pot method and incorporated as a chain extender into the SMPU matrix, endowing the material with self-healing property. The nanocarbon spheres (CS) with photothermal conversion effect were dispersed into SMPU/UPy to obtain a self-healing SMPU composite. In order to examine the photothermal-induced shape memory behavior of SMPU/UPy/CS, the SMPU was folded to form a temporary windmill shape. The temporary windmill shape was progressively recovered to its initial flat shape by sequentially irradiating the selected material area under NIR light, as shown in Fig. 14ii. The results demonstrated that low amount of CS and the limited molecular movement resulted in low shape recovery efficiency. Additionally, the prepared material showed shape memory-assisted self-healing properties by irradiating the crack area through NIR light. The surface crack (100 μm) was healed within 60 s. The self-healing process of SMPU/UPy/CS involves two stages. In the first stage, the two ends of the crack were brought close together through the shape memory effect. During the process of prefabricating damages, the shape of the material changed, storing a certain amount of conformation entropy at both ends of the crack.[87,88] Under NIR-induced photothermal effects, this conformational entropy was released, quickly bringing the crack ends into spatial proximity (Fig. 14iv). In the second stage, the movement of molecular chains, driven by surface energy/tension, facilitates heating.[89,90] Surface tension at the unhealed interface causes the molecular chains to move towards the direction of surface tension under photothermal-induced heat stimulation, making the crack shallow and wide until closed. Once the crack was being closed, the molecular chains on the fracture surface further diffused and entangled (Fig. 14v), completing the self-healing process. Small cracks could achieve fast repair due to the shape memory effect (crack size < 300 μm). The authors also reported that the repair efficiency of NIR light (10 s) was greater than thermal-induced repair (5 min) in achieving 10% self-healing efficiency. Meanwhile, the addition of CS not only improved the photothermal effect, it also further enhanced the SMPU anti-corrosion performance through hydrophobicity and maze effect. The coating of SMPU/UPy/CS with superior self-healing and anti-corrosion properties has demonstrated its significant potential in industrial applications.

Alternatively, polymeric materials such as polyaniline (PANI) have also been found to exhibit photothermal conversion properties. PANI has been studied in diverse fields of applications such as composite films,[91] porous material,[92] and

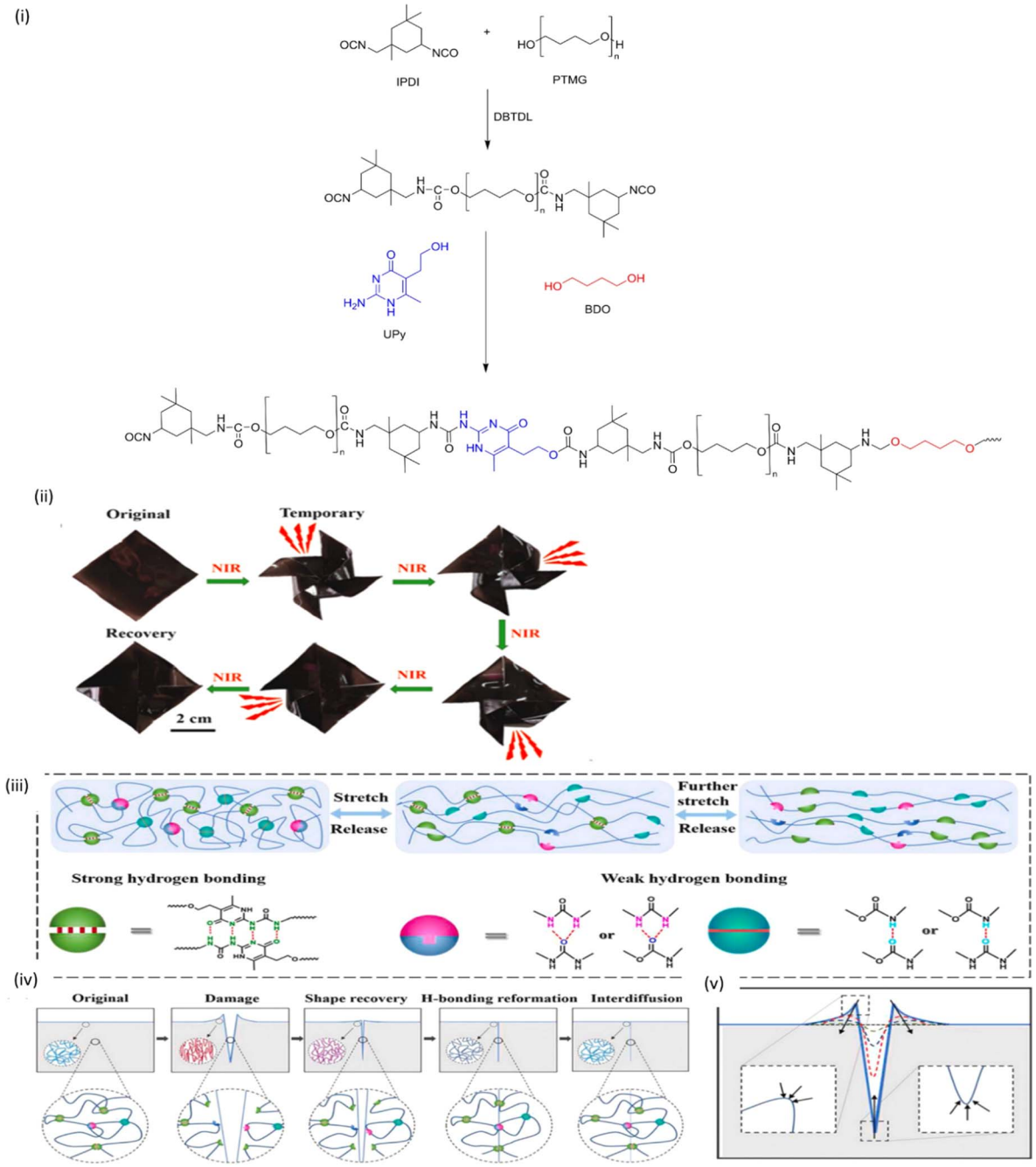

Fig. 14 (i) Reaction scheme of SMPU/UPy; (ii) photograph of shape memory recovery process of SMPU/UPy/CS under NIR light, and self-healing mechanism diagram: (iii) hierarchical H-bonding in the SMPU/UPy; schematic diagram of the self-healing mechanism of SMPU/UPy/CS under (iv) shape memory effect and (v) illustration of action of energy/tension. Readapted with permission.[44] Copyright 2024, Elsevier.

photothermal therapy.[93] PANI was being incorporated into SMPU matrix to provide photothermal properties to the host polymer. Zhang and co-researchers (2024) reported on the preparation of phosphotungstic acid modified polyaniline-polyurethane composite (SMPU/PWPA) by reacting TDI, polyethylene oxide (PEO, $M_w = 100\,000$ g mol^{-1}) and poly(propylene glycol)-*block*-poly(ethylene glycol)-*block*-poly(propylene glycol) (PPG–PEG–PPG, $M_w = 2000$ g mol^{-1}), followed by the incorporation of phosphotungstic acid doped polyaniline (PWPA)[94] *via in situ* polymerization (Fig. 15i).[45,95] PANI was responsible for photothermal effect, while phosphotungstic acid acted as a photothermal effect enhancer. The introduction of PWPA led to an increase of T_g to 52.7 °C in SMPU/PWPA due to the cross-linking effect of PWPA. Under the irradiation of NIR laser (808 nm, 1.5 W cm^{-2}, BluePrint, China), the modified PANI converted light energy into thermal energy and thus softened the epoxy moieties to trigger the shape memory effect of PU. The photothermal induced shape memory behavior also facilitated

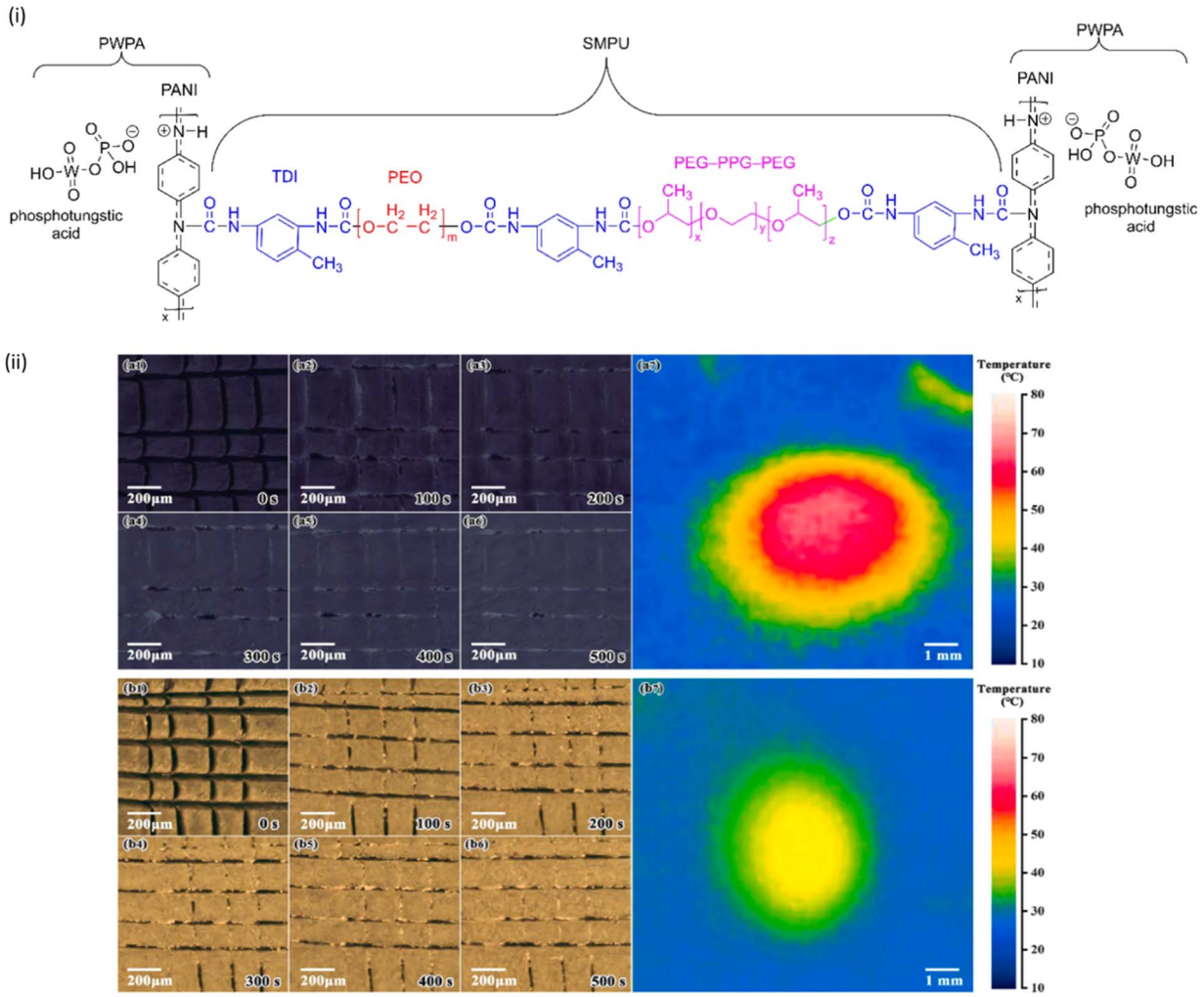

Fig. 15 (i) Chemical structure of the prepared SMPU/PWPA;[64] (ii) optical photographs and infrared thermal images of scratched (a) SMPU/PWPA, and (b) SMPU coatings under NIR laser irradiation for 500 s. Readapted with permission.[45] Copyright 2023, Elsevier.

the closure and repair of the damaged coating. As shown in Fig. 15ii, the SMPU/PWPA generated a higher local surface temperature (~70 °C) compared to SMPU coating (~40 °C). This enhanced photothermal effect facilitated the healing of scratches in the SMPU/PWPA, whereas the neat SMPU coating remained unchanged. The increased local temperature enhanced the mobility of polymer chains in both the SMPU/PWPA and epoxy resin, leading to the softening of the coating near the scratch. The relatively cold and hardened polymer on the periphery aided in healing the softened coating near the scratch area through thermal expansion. The active polymer chains of SMPU and epoxy resin entangled, diffused and repaired the damaged coating. These results suggested the SMPU/PWPA has the potential to be used in marine and aerospace corrosion protection applications.

On the other hand, a photothermal-responsive antibacterial bio-based SMPU was prepared by the reaction of castor oil-based polyols, MDI and 1,4-benzoquinone dioxime (BQDO) as photothermal agent.[46] The BQDO reacted with isocyanate to form dynamic oxime–carbamate bonds, which had improved the mechanical properties of the biobased SMPU. NIR light was used to evaluate the photothermal-responsive shape memory properties of the synthesized SMPU. As shown in Fig. 16, the local area of the SMPU strip was irradiated by NIR light to enable precise heating and thus its shape was changed to 'V' shape. The SMPU strip was temporarily fixed after removing the NIR source. The V-shape SMPU strip was able to recover to its initial shape under NIR illumination within 30 s. The authors also highlighted the evaluation of photothermal antibacterial properties of SMPU against *Escherichia coli* and *Staphylococcus aureus* by colony-forming unit method. The SMPU demonstrated excellent antibacterial activity with more than 98%

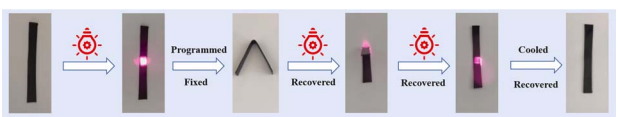

Fig. 16 Visualization of the BPU-2 photothermal shape memory effect at an irradiation intensity of 0.8 W cm^{-2}. Readapted with permission.[46] Copyright 2023, Elsevier.

sterilization rate against both bacteria. Under NIR irradiation (0.8 W cm^{-2}), the SMPU could reach high temperature (102.1 °C) within 50 s and thus achieved the high-temperature sterilization. The synthesized biobased SMPU has shown its great potential in the application of biomedical material and devices.

Bio-based photothermal agent-containing SMPU

Natural pigment can also be employed to absorb light and convert it into heat in SMPU matrix. For instance, melanin, a natural pigment found in microorganisms, plants and animals, is well-known for its photoprotective properties.[96] Melanin efficiently absorbs a wide range of radiation, from UV to IR, and dissipates the absorbed light energy as heat.[97] Xie *et al.* (2020) reported the extraction of natural melanin (YM) (Fig. 17) pigment from yak hair waste and its incorporation into SMPU for fabricating NIR-induced photothermal SMPU implants.[47] The YM was added into SMPU matrix, serving as a photothermal filler to increase the temperature over T_{trans} (~65 °C) under NIR light illumination, thereby inducing the shape memory effect of the SMPU. The SMPU/YM was fabricated into two different thickness (0.1 mm and 1 mm), where the thin film was folded while the thick film was rolled and elongated at 90 °C, followed by cooling at room temperature for temporary shape fixation. Under NIR light irradiation (845 nm, 8.77 W cm^{-2}, NIR LED chip), both folded and rolled SMPU/YM films were gradually returned to their original shapes (flat), which demonstrated the photothermal-induced shape memory recovery process. The SMPU/YM also exhibited excellent photostability, where the photothermal effect did not compromise after 5 cycles of NIR light irradiation. It is also noted that the temperature of the films reduced quickly due to fast heat transfer from YM and homogenous dispersion of YM particle in the SMPU. Furthermore, the prepared SMPU/YM composites exhibited low toxicity to both mouse fibroblast cells (L929) cells and human mesenchymal stem cells (hMSCs) *in vitro*. Additionally, the composites demonstrated biostability, with low degradation (maintained at ~99%) in the PBS solution for 12 weeks. The SMPU/YM film was fabricated to column into a column using a self-made tubular Teflon mold and proposed as a contraceptive device to be implanted in the fallopian tube. This elongated column was able to return to its initial size *in vivo* within 60 s under low NIR laser intensity (808 nm, 0.5 W cm^{-2}). It is well noted that the NIR laser intensity used is much lower than the general laser intensity for photothermal cancer therapy (808 nm, 1–2 W cm^{-2}).[98] The non-toxic, biostable, biocompatible nature of the SMPU/YM, along with their fast shape recovery performance, highlighted their potential as a smart and long-term implant material.

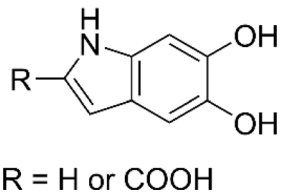

Fig. 17 The chemical structure of melanin from yak hair.

Conclusions and future aspects

In this review, we explored various photothermal agents incorporated into the SMPU matrix to impart responsiveness to NIR light. The thermal-induced shape memory properties inherent to PU, combined with NIR light responsiveness, offer synergistic advantages for biomedical applications, such as bone repairing, hemostatic materials, intestinal stents and contraceptive implant materials. To enhance understanding, reaction schemes and schematic illustrations are included to illustrate the NIR light-induced shape memory effect of PU by the photothermal effect. NIR-light is particularly attractive as a stimulus due to its availability and superior penetration power as compared to other light sources. However, the intensity of NIR light must be carefully considered when used in direct exposure to biological system.

Despite the extraordinary photothermal effects, issues such as unsatisfactory mechanical properties at high photothermal agent concentration and long-term safety concerns of these synthetic materials remain major challenges. For instance, carbon-based nanomaterials can induce oxidative stress and lung inflammation after administration, while metallic nanoparticles might cause metal-related cytotoxicity in biological systems. Addressing the cytotoxicity and potential risks of photothermal agents requires careful consideration of their concentration in the host SMPU and the intensity of NIR light.

To mitigate oxidative stress and inflammation caused by carbon-based nanomaterials, surface modifications could be explored to reduce direct contact with biological tissues.[99] Additionally, exploring the photothermal properties of biocompatible metallic nanoparticles, such as gold nanoparticles,[100] could address the cytotoxicity induced by metallic nanoparticles and provide a safer alternative for photothermal applications in SMPU.

The use of bio-based photothermal agents in SMPU remains largely unexplored. Investigating natural compounds with photothermal properties, such as porphyrin compounds and chlorophyll,[101] could lead to promising alternatives. These materials may offer photothermal effects without the associated cytotoxicity observed with synthetic agents. Bio-based photothermal agents not only ensure biosafety but also address environmental and sustainability concerns.

Efforts are also required to enhance the mechanical strength of SMPU composites without compromising their photothermal performance. Investigation on novel composite formulations, reinforcement strategies, and processing techniques to enhance the mechanical strength of SMPUs without compromising their photothermal performance is required. Investigation on novel composite formulations, reinforcement strategies, and processing techniques to enhance the mechanical strength of SMPUs without compromising their photothermal performance is required. Reducing reliance on petrochemical-based starting reactants in SMPU by exploring greener alternatives that

minimize environmental impact is a critical step forward. Exploring new applications for photothermal SMPU beyond biomedical uses, such as smart textiles, soft robotics, and environmental remediation, is crucial to unlock the full potential of photothermal-responsive SMPU materials, leading to safer, efficient, and sustainable solutions for a wide range of medical and industrial applications.

Data availability

This review article, entitled "NIR-induced photothermal-responsive shape memory polyurethane for versatile smart material applications" is based on previously published studies and data. All data referenced in this review are available from the original sources, which are cited throughout the article. Researchers interested in accessing the data should refer to the individual studies cited in the reference list for further information. No new data were generated or analyzed in this study.

Author contributions

Ki Yan, Lam: investigation, methodology, visualization, writing – original draft & editing. Choy Sin, Lee: conceptualization, methodology, visualization, supervision, investigation, writing – review & editing. Rachel Yie Hang, Tan: investigation, methodology, writing-original draft.

Conflicts of interest

There are no conflicts to declare.

Acknowledgements

The authors would like to acknowledge the Fundamental Research Grant Scheme (FRGS) (Grant No. FRGS/1/2019/STG07/IMU/02/1) and IMU University Institute for Research Development & Innovation for financial support.

References

1 Y. Tian, Z. Xu, H. Qi, X. Lu, T. Jiang, L. Wang, G. Zhang, R. Xiao and H. Wu, *Soft Matter*, 2024, **20**, 5314–5323.
2 M. Qu, H. Wang, Q. Chen, L. Wu, P. Tang, M. Fan, Y. Guo, H. Fan and Y. Bin, *Chem. Eng. J.*, 2022, **427**, 131648.
3 B. Kumar, N. Noor, S. Thakur, N. Pan, H. Narayana, S. C. Yan, F. Wang and P. Shah, *ACS Omega*, 2019, **4**, 15348–15358.
4 X. Gong, L. Liu, Y. Liu and J. Leng, *Smart Mater. Struct.*, 2016, **25**, 35036.
5 C. Russo, J. L. Ramírez, X. Fernández-Francos and S. De la Flor, *Polym. Adv. Technol.*, 2022, **33**, 1715–1726.
6 T. Li, J. Sun, J. Leng and Y. Liu, *J. Compos. Mater.*, 2022, **56**, 1725–1736.
7 S. M. Hong, J. R. Cha and J. G. Kim, *Polym. Test.*, 2020, **91**, 106852.
8 M. Staszczak, M. Nabavian Kalat, K. M. Golasiński, L. Urbański, K. Takeda, R. Matsui and E. A. Pieczyska, *Polymers*, 2022, **14**, 4775.
9 T. Yang, M. Wang, F. Jia, X. Ren and G. Gao, *J. Mater. Chem. C*, 2020, **8**, 2326–2335.
10 Shape Memory Polymer Market Size, Share & Trends Analysis Report By Material (Epoxy, PU, PLA), By End-use (Medical, Automotive, Textile, Aerospace, Construction), By Region, And Segment Forecasts, 2023–2030, **https://www.grandviewresearch.com/industry-analysis/shape-memory-polymers-market-report#**.
11 W. Shen, J. Liu, B. Du, H. Zhuo and S. Chen, *J. Mater. Chem. A*, 2021, **9**, 15087–15094.
12 D. Jang, C. B. Thompson, S. Chatterjee and L. T. J. Korley, *Mol. Syst. Des. Eng.*, 2021, **6**, 1003–1015.
13 J. Li, Z. Liang, X. Zhang and Q. Kan, *Polymer*, 2021, **237**, 124337.
14 F. Li, Y. Liu and J. Leng, *Smart Mater. Struct.*, 2019, **28**, 103003.
15 B. S. Lee, B. C. Chun, Y.-C. Chung, K. Il Sul and J. W. Cho, *Macromolecules*, 2001, **34**, 6431–6437.
16 H.-H. Wang and U.-E. Yuen, *J. Appl. Polym. Sci.*, 2006, **102**, 607–615.
17 V. D. Punetha, Y. M. Ha, Y. O. Kim, Y. C. Jung and J. W. Cho, *Sens. Actuators, B*, 2020, **321**, 128468.
18 X. Zhou, G. Wang, D. Li, Q. Wang, K. Zhu, Y. Hao, Y. Xu and N. Li, *Composites, Part A*, 2024, **177**, 107920.
19 Y. Chen, X. Zhao, Y. Li, Z. Y. Jin, Y. Yang, M. B. Yang and B. Yin, *J. Mater. Chem. C*, 2021, **9**, 5515–5527.
20 S. Aslan and S. Kaplan, *Fibers Polym.*, 2018, **19**, 272–280.
21 N. Beshchasna, M. Saqib, H. Kraskiewicz, Ł. Wasyluk, O. Kuzmin, O. C. Duta, D. Ficai, Z. Ghizdavet, A. Marin, A. Ficai, Z. Sun, V. F. Pichugin, J. Opitz and E. Andronescu, *Pharmaceutics*, 2020, **12**, 349.
22 R. Yang, W. Liu, A. Wang, X. Deng, Y. Feng, Q. Zhang, Z. Li, F. Luo, J. Li and H. Tan, *J. Mater. Chem. B*, 2022, **10**, 8918–8930.
23 B. Zeng, Y. Li, L. Wang, Y. Zheng, J. Shen and S. Guo, *ACS Sustain. Chem. Eng.*, 2020, **8**, 1538–1547.
24 Y. Q. Fu, W. M. Huang, J. K. Luo and H. Lu, *Woodhead Publ. Ser. Biomater.*, 2015, 167–195.
25 Y. Zhu, J. Hu, L.-Y. Yeung, Y. Liu, F. Ji and K. Yeung, *Smart Mater. Struct.*, 2006, **15**, 1385.
26 C. Li, J. Zhong, H. Jiang and P. Shi, *Dalton Trans.*, 2022, **51**, 16757–16763.
27 N. M. Vlasov and I. I. Fedik, *Journal of Thermal Stresses*, 2009, **32**, 755–767.
28 N. Ahmed, M. Atif, N. Ahmed, F. Iftikhar, S. Nauman and B. Niaz, *Polym. Polym. Compos.*, 2022, **30**, 09673911221076847.
29 H. Xie, J. Shao, Y. Ma, J. Wang, H. Huang, N. N. Yang, H. Wang, C. Ruan, Y. Luo, Q.-Q. Wang, P. K. P. K. Chu and X.-F. X.-F. Yu, *Biomaterials*, 2018, **164**, 11–21.
30 M. V Padalkar and N. Pleshko, *Analyst*, 2015, **140**, 2093–2100.
31 H. Lv, H. Chi, X. Yang, J. Peng, W. Wang and D. Tang, *Colloids Surf., A*, 2021, **627**, 127100.

32 L. Yang, R. Tong, Z. Wang and H. Xia, *ChemPhysChem*, 2018, **19**, 2052–2057.
33 S. Dai, S. Yue, Z. Ning, N. Jiang and Z. Gan, *ACS Appl. Mater. Interfaces*, 2022, **14**, 14668–14676.
34 F. Sang, L. Pan, Z. Ji, B. Zhang, Z. Meng, L. Cao, J. Zhang, X. Li, X. Yang and C. Shi, *Colloids Surf., B*, 2023, **232**, 113590.
35 Y. Zhang, C. Li, W. Zhang, J. Deng, Y. Nie, X. Du, L. Qin and Y. Lai, *Bioact. Mater.*, 2022, **16**, 218–231.
36 Y. Liu, Z. Zhang, K. Yang, D. Chen and Z. Li, *Polymer*, 2022, **247**, 124749.
37 Y. Bai, J. Zhang, D. Wen, P. Gong, J. Liu, J. Ju and X. Chen, *Compos. Sci. Technol.*, 2020, **187**, 107940.
38 W. Du, Y. Jin, S. Lai, L. Shi, Y. Shen and H. Yang, *Composites, Part A*, 2020, **128**, 105686.
39 W. Du, Y. Jin, L. Shi, Y. Shen, S. Lai and Y. Zhou, *Composites, Part B*, 2020, **195**, 108092.
40 V. D. Punetha, Y. M. Ha, Y. O. Kim, Y. C. Jung and J. W. Cho, *Polymer*, 2019, **181**, 121791.
41 P. Yan, W. Zhao, L. Jiang, B. Wu, K. Hu, Y. Yuan and J. Lei, *J. Appl. Polym. Sci.*, 2017, **135**, 1–8.
42 Y. M. Ha, Y. O. Kim, Y. N. Kim, J. Kim, J. S. Lee, J. W. Cho, M. Endo, H. Muramatsu, Y. A. Kim and Y. C. Jung, *Composites, Part B*, 2019, **175**, 1–7.
43 R. Yang, W. Liu, N. Song, X. Li, Z. Li, F. Luo, J. Li and H. Tan, *Macromol. Rapid Commun.*, 2022, **43**, 1–12.
44 Q. Zhang, A. Ma, B. Zhang, S. Liang, Y. Chen, Q. Li, X. Mao, W. Zhao and H. Zhou, *Polymer*, 2024, **299**, 126957.
45 X. q. Zhang, R. Ding, J. Lv, Y. c. Zhang, A. l. Ji, J. Fu, X. Lv, S. y. Yang, L. Yao, X. Liang, J. Liu and H. b. Yu, *J. Ind. Eng. Chem.*, 2024, **134**, 194–206.
46 X. Wang, X. Huang, Z. Ji, W. Hu, H. Sheng and X. Li, *Ind. Crops Prod.*, 2023, **206**, 117628.
47 W. Xie, F. Yan, E. Pakdel, J. Sharp, D. Liu, X. Wang, S. Zhan and L. Sun, *ACS Biomater. Sci. Eng.*, 2020, **6**, 5305–5314.
48 T. Liu, K. C. Kim, B. Lee, Z. Chen, S. Noda, S. S. Jang and S. W. Lee, *Energy Environ. Sci.*, 2017, **10**, 205–215.
49 X. Hu, Y. Ke, M. Zhang, H. Niu, D. Wu and L. Zhao, *High Perform. Polym.*, 2021, **33**, 601–614.
50 G. Liu, N. Gao, Y. Zhou, J. Nie, W. Cheng, M. Luo, L. Mei, X. Zeng and W. Deng, *Pharmaceutics*, 2019, **11**, 507.
51 H. Zhang, H. Xia and Y. Zhao, *ACS Macro Lett.*, 2014, **3**, 940–943.
52 Z. Cao, R. Wang, L. Hao, W. Jiao, F. Yang, Q. Wang, W. Liu, B. Zhang, X. Lu and X. He, *RSC Adv.*, 2015, **5**, 5680–5685.
53 Y. Liu, K. Ai, J. Liu, M. Deng, Y. He and L. Lu, *Adv. Mater.*, 2013, **25**, 1353–1359.
54 T. Xie, *Nature*, 2010, **464**, 267–270.
55 Y. Zou, X. Chen, P. Yang, G. Liang, Y. Yang, Z. Gu and Y. Li, *Sci. Adv.*, 2020, **6**, 1–9.
56 Q. Duan, J. Wang, B. Zhang, X. Wang, J. Xue, W. Zhang and S. Sang, *Colloids Surf., B*, 2022, **210**, 112247.
57 L. Yang, X. Lu, Z. Wang and H. Xia, *Polym. Chem.*, 2018, **9**, 2166–2172.
58 Y. Liu, K. Ai and L. Lu, *Chem. Rev.*, 2014, **114**, 5057–5115.
59 L. Tan, J. Li, X. Liu, Z. Cui, X. Yang, S. Zhu, Z. Li, X. Yuan, Y. Zheng, K. W. K. Yeung, H. Pan, X. Wang and S. Wu, *Adv. Mater.*, 2018, **30**, 1801808.
60 X. Zhang, Y. Peng, X. Wang and R. Ran, *ACS Appl. Polym. Mater.*, 2021, **3**, 1899–1911.
61 R. J. Thomas, B. A. Rockwell, W. J. Marshall, R. C. Aldrich, S. A. Zimmerman and R. J. Rockwell Jr, *J. Laser Appl.*, 2002, **14**, 57–66.
62 P. Liu, H. Lai, X. Luo, Q. Xia, D. Zhang, Z. Cheng, Y. Liu and L. Jiang, *ACS Nano*, 2020, **14**, 14047–14056.
63 H. Liu, Y. Shi, B. Tang, T. Wang and H. Zhang, *Mater. Res. Express*, 2021, **8**, 035903.
64 C. Jia, F. Zhang, J. Lin, L. Feng, T. Wang, Y. Feng, F. Yuan, Y. Mai, X. Zeng and Q. Zhang, *J. Nanobiotechnol.*, 2022, **20**, 90.
65 Z. Guo, H. Zhang, S. Lu, Z. Wang, S. Tang, J. Shao, Z. Sun, H. Xie, H. Wang, X.-F. Yu and P. K. Chu, *Adv. Funct. Mater.*, 2015, **25**, 6996–7002.
66 Y. Zhang, J. Xu, Y. C. Ruan, M. K. Yu, M. O'Laughlin, H. Wise, D. Chen, L. Tian, D. Shi, J. Wang, S. Chen, J. Q. Feng, D. H. K. Chow, X. Xie, L. Zheng, L. Huang, S. Huang, K. Leung, N. Lu, L. Zhao, H. Li, D. Zhao, X. Guo, K. Chan, F. Witte, H. C. Chan, Y. Zheng and L. Qin, *Nat. Med.*, 2016, **22**, 1160–1169.
67 Y. Liu, Z. Zhang, J. Wang, T. Xie, L. Sun, K. Yang and Z. Li, *Polymer*, 2021, **228**, 123860.
68 J. Zeng, M. Cheng, Y. Wang, L. Wen, L. Chen, Z. Li, Y. Wu, M. Gao and Z. Chai, *Adv. Healthcare Mater.*, 2016, **5**, 772–780.
69 H. Dong, Y. Wen, J. Lin, X. Zhuang, R. Xian, P. Li and S. Li, *J. Funct. Biomater.*, 2023, **14**, 284.
70 Y. Liu, X. Li, S. Xiao, X. Liu, X. Chen, Q. Xia, S. Lei, H. Li, Z. Zhong and K. Xiao, *Int. J. Nanomed.*, 2020, **15**, 9499–9514.
71 P. Xiong, X. Huang, N. Ye, Q. Lu, G. Zhang, S. Peng, H. Wang and Y. Liu, *Adv. Sci.*, 2022, **9**, e2106049.
72 A. H. Faid, M. A. Rafea, S. Gad, M. Sharaky and M. A. Ramadan, *Cancer Nanotechnol.*, 2024, **15**, 17.
73 K. Tadyszak, J. K. Wychowaniec and J. Litowczenko, *Nanomaterials*, 2018, **8**, 944.
74 N. Van Herck and F. E. Du Prez, *Macromolecules*, 2018, **51**, 3405–3414.
75 S. Ji, W. Cao, Y. Yu and H. Xu, *Adv. Mater.*, 2015, **27**, 7740–7745.
76 Y. Ouyang, Z. Cao, X. Chen, S. Lu, H. Ruan, X. Xu and Y. Li, *J. Polym. Res.*, 2022, **29**, 1–10.
77 X. Chen, Y. Liu, J. Li, T. W. Wong, T. Chen, T. Zhang and L. Wang, *Polym. Test.*, 2023, **122**, 108026.
78 J. P. Coyle, R. C. Derk, T. G. Kornberg, D. Singh, J. Jensen, S. Friend, R. Mercer, T. A. Stueckle, P. Demokritou, Y. Rojanasakul and L. W. Rojanasakul, *Part. Fibre Toxicol.*, 2020, **17**, 40.
79 V. Vijayalakshmi, B. Sadanandan and R. V Anjanapura, *J. Biochem. Mol. Toxicol.*, 2023, **37**, e23283.
80 N. M. Anahita, F. Omid and M. H. Mohammad, *Recent Pat. Biotechnol.*, 2023, **17**, 186–195.
81 *Clinical Biochemistry of Domestic Animals*, ed. J. J. Kaneko, J. W. Harvey and M. L. Bruss, Academic Press, 1997.

82 X. Li, W. Liu, Y. Li, W. Lan, D. Zhao, H. Wu, Y. Feng, X. He, Z. Li, J. Li, F. Luo and H. Tan, *J. Mater. Chem. B*, 2020, **8**, 5117–5130.
83 J. W. Li, W. C. Tsen, C. H. Tsou, M. C. Suen and C. W. Chiu, *Polymers*, 2019, **11**, 1333.
84 H. S. Lee, Y. K. Wang and S. L. Hsu, *Macromolecules*, 1987, **20**, 2089–2095.
85 K. J. Cha, E. Lih, J. Choi, Y. K. Joung, D. J. Ahn and D. K. Han, *Macromol. Biosci.*, 2014, **14**, 667–678.
86 J. T. Hong, T. J. Kim, S. N. Hong, Y.-H. Kim, D. K. Chang and E. R. Kim, *Sci. Rep.*, 2020, **10**, 19841.
87 T. Chen, L. Fang, X. Li, D. Gao, C. Lu and Z. Xu, *Prog. Org. Coat.*, 2020, **147**, 105876.
88 C. C. Hornat and M. W. Urban, *Prog. Polym. Sci.*, 2020, **102**, 101208.
89 X. Luo and P. T. Mather, *ACS Macro Lett.*, 2013, **2**, 152–156.
90 C. C. Hornat and M. W. Urban, *Nat. Commun.*, 2020, **11**, 1028.
91 B. Butoi, C. S. Ciobanu, S. L. Iconaru, C. C. Negrilă, M. A. Badea, M. Balas, A. Dinischiotu, G. Predoi, B. Bita, A. Groza and D. Predoi, *Polymers*, 2022, **14**, 1821.
92 J. Oh, Y. K. Kim, J. S. Lee and J. Jang, *Nanoscale*, 2019, **11**, 6462–6470.
93 J. Zhou, Z. Lu, X. Zhu, X. Wang, Y. Liao, Z. Ma and F. Li, *Biomaterials*, 2013, **34**, 9584–9592.
94 Y. Yao, H. Sun, Y. Zhang and Z. Yin, *Prog. Org. Coat.*, 2020, **139**, 105470.
95 R. Sattar, A. Kausar and M. Siddiq, *Chin. J. Polym. Sci.*, 2015, **33**, 1313–1324.
96 A. N. Tran-Ly, C. Reyes, F. W. M. R. Schwarze and J. Ribera, *World J. Microbiol. Biotechnol.*, 2020, **36**, 170.
97 J. Roldan-Kalil, L. Zueva, J. Alves, V. Tsytsarev, P. Sanabria and M. Inyushin, *Photochem. Photobiol.*, 2023, **99**, 1092–1096.
98 S. Sharma, S. Batra, M. K. Chauhan and V. Kumar, in *Targeted Cancer Therapy in Biomedical Engineering*, ed. R. Malviya and S. Sundram, Springer Nature, Singapore, 2023, pp. 755–780.
99 A. Khan and K. A. Alamry, in *Surface Modified Carbon Nanotubes Volume 1: Fundamentals, Synthesis and Recent Trends*, American Chemical Society, 2022, vol. 1424, p. 1.
100 W. Yang, B. Xia, L. Wang, S. Ma, H. Liang, D. Wang and J. Huang, *Materials Today Sustainability*, 2021, **13**, 100078.
101 J. Lin and D. Shi, *Appl. Phys. Rev.*, 2021, **8**, 11302.